19. Seino Y, Ikeda M, Kurahachi H, *et al.* Failure of suppress plasma glucagon concentrations by orally administered glucose in diabetic patients after treatment. *Diabetes* 1978; 27: 1145–1150.
20. Kosaka K, Kuzuya T, Akanuma Y, *et al.* Increase in insulin response after treatment of overt maturity-onset diabetes is independent of the mode of treatment. *Diabetologia* 1980; 18: 23–28.
21. Iwasaki Y, Kondo K, Hasegawa H, *et al.* C-peptide response to glucagon in type 2 diabetes mellitus: a comparison with oral glucose tolerance test. *Diabetes Res* 1994; 25: 129–137.
22. Rossetti L, Giaccari A, DeFronzo RA. Glucose toxicity. *Diabetes Care* 1990; 13: 610–630.
23. Knop FK, Vilsbøll T, Højberg PV, *et al.* Reduced incretin effect in type 2 diabetes: cause or consequence of the diabetic state? *Diabetes* 2007; 56: 1951–1959.
24. Højberg PV, Vilsbøll T, Zander M, *et al.* Four weeks of near-normalization of blood glucose has no effect on postprandial GLP-1 and GIP secretion, but augments pancreatic B-cell responsiveness to a meal in patients with Type 2 diabetes. *Diabet Med* 2008; 25: 1268–1275.
25. Fujimoto S, Nabe K, Takehiro M, *et al.* Impaired metabolism-secretion coupling in pancreatic β-cells: role of determinants of mitochondrial ATP production. *Diabetes Res Clin Pract* 2007; 77(Suppl. 1): S2–S10.
26. Mukai E, Fujimoto S, Sato H, *et al.* Exendin-4 suppresses Src activation and reactive oxygen species production in diabetic GK rat islets in an Epac-dependent manner. *Diabetes* 2011; 60: 218–226.
27. Meier JJ, Menge BA, Breuer TG, *et al.* Functional assessment of pancreatic β-cell area in humans. *Diabetes* 2009; 58: 1595–1603.

 © 2011 Asian Association for the Study of Diabetes and Blackwell Publishing Asia Pty Ltd

JDI Journal of Diabetes Investigation Open access
Official Journal of the Asian Association for the Study of Diabetes
ORIGINAL ARTICLE

Palmitate induces reactive oxygen species production and β-cell dysfunction by activating nicotinamide adenine dinucleotide phosphate oxidase through Src signaling

Yuichi Sato[1], Shimpei Fujimoto[1,2], Eri Mukai[1], Hiroki Sato[1], Yumiko Tahara[1], Kasane Ogura[1], Gen Yamano[1], Masahito Ogura[1], Kazuaki Nagashima[1], Nobuya Inagaki[1]*

[1]Department of Diabetes and Clinical Nutrition, Graduate School of Medicine, Kyoto University, Kyoto, and [2]Department of Endocrinology, Metabolism and Nephrology, Kochi Medical School, Kochi University, Nankoku, Japan

Keywords
Lipotoxicity, Pancreatic β-cells, Reactive oxygen species

***Correspondence**
Nobuya Inagaki Tel.: +81-75-751-3560
Fax: +81-75-751-4244
E-mail address: inagaki@metab.kuhp.kyoto-u.ac.jp

J Diabetes Invest 2014; 5: 19–26

doi: 10.1111/jdi.12124

ABSTRACT

Aims/Introduction: Chronic hyperlipidemia impairs pancreatic β-cell function, referred to as lipotoxicity. We have reported an important role of endogenous reactive oxygen species (ROS) overproduction by activation of Src, a non-receptor tyrosine kinase, in impaired glucose-induced insulin secretion (GIIS) from diabetic rat islets. In the present study, we investigated the role of ROS production by Src signaling in palmitate-induced dysfunction of β-cells.

Materials and Methods: After rat insulinoma INS-1D cells were exposed to 0.6 mmol/L palmitate for 24 h (palmitate exposure); GIIS, ROS production and nicotinamide adenine dinucleotide phosphate oxidase (NOX) activity were examined with or without exposure to10 μmol/L 4-amino-5-(4-chlorophenyl)-7-(t-butyl)pyrazolo[3,4-d]pyrimidine (PP2), a Src inhibitior, for 30 or 60 min.

Results: Exposure to PP2 recovered impaired GIIS and decreased ROS overproduction as a result of palmitate exposure. Palmitate exposure increased activity of NOX and protein levels of NOX2, a pathological ROS source in β-cells. Palmitate exposure increased the protein level of $p47^{phox}$, a regulatory protein of NOX2, in membrane fraction compared with control, which was reduced by PP2. Transfection of small interfering ribonucleic acid of *$p47^{phox}$* suppressed the augmented $p47^{phox}$ protein level in membrane fraction, decreased augmented ROS production and increased impaired GIIS by palmitate exposure. In addition, exposure to PP2 ameliorated impaired GIIS and decreased ROS production in isolated islets of KK-A^y mice, an obese diabetic model with hyperlipidemia.

Conclusions: Activation of NOX through Src signaling plays an important role in ROS overproduction and impaired GIIS caused by chronic exposure to palmitate, suggesting a lipotoxic mechanism of β-cell dysfunction of obese mice.

INTRODUCTION

In pancreatic β-cells, glucose metabolism regulates exocytosis of insulin granules through metabolism-secretion coupling[1]. Reactive oxygen species (ROS) is one of the most important factors that impair glucose-induced insulin secretion (GIIS) in β-cells.

Exposure to exogenous hydrogen peroxide (H_2O_2), the most abundant ROS, reduces glucose-induced insulin secretion by impairing mitochondrial metabolism in β-cells[2,3]. ROS are normal byproducts of glucose metabolism, including glycolysis and mitochondrial oxidative phosphorylation[4]. In β-cells, ROS

Received 1 March 2013; revised 20 May 2013; accepted 28 May 2013

© 2013 The Authors. Journal of Diabetes Investigation published by Asian Association for the Study of Diabetes (AASD) and Wiley Publishing Asia Pty Ltd
This is an open access article under the terms of the Creative Commons Attribution-NonCommercial-NoDerivs License, which permits use and distribution in any medium, provided the original work is properly cited, the use is non-commercial and no modifications or adaptations are made.

production through non-mitochondrial and mitochondrial pathways has been proposed. In the mitochondrial pathway, ROS is generated in the electron transport chain associated with the mitochondrial membrane potential[5]. However, in pathophysiological conditions, nicotinamide adenine dinucleotide phosphate (NADPH) oxidase (NOX), an important non-mitochondrial ROS source, could play an important role in ROS generation in β-cells[6].

Deleterious effects of chronic hyperlipidemia on β-cell function are referred to as lipotoxicity[7]. Chronic exposure to palmitate, a long-chain saturated fatty acid, impairs GIIS with an increase in production of ROS in β-cells[8,9]. Recently, an important role of NOX in ROS production in β-cells by palmitate exposure has been proposed[10]. In addition, both oxidative stress markers and NOX expression are increased in islets of obese diabetic rodents with hyperlipidemia[11,12]. We have proposed that endogenous overproduction of ROS involving activation of Src, a non-receptor tyrosine kinase, plays an important role in impaired metabolism-secretion coupling in islets of diabetic Goto–Kakizaki (GK) rats[13–15]. An important role of Src in activation of NOX has been reported in various cells[16,17]. In the present study, to elucidate the mechanism of lipotoxicity in β-cells more precisely, we investigated involvement of Src in ROS production derived from NOX and impaired GIIS caused by chronic exposure to palmitate.

MATERIALS AND METHODS

Materials

Palmitate obtained from Nacalai (Kyoto, Japan) was dissolved in 95% ethanol at stock concentration of 100 mmol/L. The specific Src inhibitor, 4-amino-5-(4-chlorophenyl)-7-(t-butyl)pyrazolo[3,4-d]pyrimidine (PP2), was purchased from Tocris (Ellisville, MO, USA).

Cell Culture and Mouse Islet Isolation

Rat insulinoma cell line INS-1D cells were cultured as previously described[18] with or without palmitate in the presence of 0.5% bovine serum albumin (BSA) for 24 h.

Male KK-A^y mice and control C57/BL6 mice (Clea Japan, Tokyo, Japan) were maintained and used in accordance with the guidelines of the animal care committee of Kyoto University. All experiments were carried out with mice aged 8–10 weeks. Pancreatic islets were isolated as previously described[19].

Insulin Secretion

Insulin secretion from INS-1D cells was determined as previously described[18]. INS-1D cells cultured on 24-well plates coated with 0.001% poly-L-ornithine were washed with Krebs–Ringer bicarbonate HEPES (KRBH) buffer composed of (in mmol/L) 140 NaCl, 3.6 KCl, 0.5 $MgSO_4$, 0.5 NaH_2PO_4, 1.5 $CaCl_2$, 2 $NaHCO_3$ and 10 HEPES (pH 7.4) with 0.1% BSA and 2 mmol/L glucose, pre-incubated at 37°C for 30 min in KRBH with 2 mmol/L glucose, and then incubated at 37°C for 30 min in KRBH with 2 mmol/L glucose and 10 mmol/L glucose. Insulin release from intact islets was measured using batch incubation using KRBH supplemented with 0.2% BSA as previously described[19].

ROS Measurements

ROS was measured according to the method previously described[20]. INS-1D cells and isolated islets were incubated in KRBH medium containing 2 mmol/L glucose and 10 μmol/L 5-(and 6-) chloromethyl-2′,7′-dichlorodihydrofluorescein diacetate (CM-H_2DCFDA; Invitrogen, Carisbad, CA, USA) for 60 min at 37°C, and then were rapidly frozen, stored at −80°C and thawed. Fluorescence of the supernatant was quantified using a reader (Powerscan HT; DS Pharma Biomedical, Suita, Japan) with excitation wavelength at 485 nm and emission at 530 nm, which was corrected by subtracting parallel blanks.

Isolation of Total Ribonucleic Acid and Quantitative Reverse Transcription Polymerase Chain Reaction

Total ribonucleic acid (RNA) was isolated from INS-1D cells using RNeasy mini kit (Qiagen, Hilden, Germany). cDNA was prepared by reverse transcriptase (Superscript II; Invitrogen) with an oligo (dT) primer. The rat sequences of forward and reverse primers to *NOX2/gp91^{phox}* and *β-actin* (as an inner control) were as follows: (*NOX2/gp91^{phox}*: 5′-TGA CTC GGT TGG CTG GCA TC-3′, 5′-CGC AAA GGT ACA GGA ACA TGG G -3′, *β-actin*: 5′- CAA TGA GCG GTT CCG ATG CC -3′, 5′- AAT GCC TGG GTA CAT GGT GG -3′). AmpliTaq Gold (Applied Biosystems, Foster, CA, USA) was used as a DNA polymerase for reverse transcription polymerase chain reaction (RT–PCR). SYBR Green PCR Master Mix (Applied Biosystems) was prepared for quantitative RT–PCR run. The thermal cycling conditions were denaturation at 95°C for 10 min followed by 40 cycles at 95°C for 30 s and 60°C for 30 s.

Immunoblot Analysis

For immunoblotting, cells were washed with phosphate-buffered saline (PBS) containing protease inhibitor cocktail (Complete; Roche, Mannheim, Germany) and phosphatase inhibitor cocktail (Calbiochem, Darmstadt, Germany), suspended in 1 mL of PBS containing protease inhibitor and phosphatase inhibitor, and homogenized as previously described[18]. Membrane fraction was prepared as described previously[21]. INS-1D cells were washed three times with PBS, suspended in buffer A consisting of 50 mmol/L Tris (pH 7.5), 1 mmol/L ethylenediaminetetraacetic acid, and containing protease inhibitor cocktail, phosphatase inhibitor cocktail and 5 mol/L sodium pyrophosphate, homogenized and then centrifuged at 10,000 *g* at 4°C for 1 h. The pellets were resuspended in 500 μL of buffer A and stored at −80°C until immunoblot analysis or NOX activity assay. Protein (20 μg per sample) was separated on a 15% polyacrylamide gel and transferred to a polyvinylidene difluoride membrane. After blocking with Tris-buffered saline

© 2013 The Authors. Journal of Diabetes Investigation published by AASD and Wiley Publishing Asia Pty Ltd

(10 mmol/L Tris/HCl and 100 mmol/L NaCl, pH 7.5) containing 0.1% Tween 20 and 5% BSA (blocking buffer) at room temperature (25°C) for 2 h, blotted membranes were incubated overnight at 4°C with anti-p418 Src antibody (Biosource, Camarillo, CA, USA) at 1:1000 dilution, anti-glyceraldehyde 3-phosphate dehydrogenase (GAPDH) antibody (Millipore, Billerica, MA, USA) at 1:1000 dilution, anti-NCF1 ($p47^{phox}$) antibody (Abcam, Cambridge, UK) at 1:1000 dilution, anti-NOX2/$gp91^{phox}$ antibody (Abcam) at 1:1000 dilution, anti-flotillin-1 antibody (Cell Signaling Technology, Danvers, MA, USA) at 1:1000 dilution in blocking buffer and subsequently with anti-rabbit or anti-mouse immunoglobulin G horseradish peroxidase-conjugated secondary antibody (GE Healthcare, Little Chalfont, UK) diluted at 1:5000 at room temperature for 2 h before detection using ECL prime™ (GE Healthcare). Band intensities were quantified with Multi Gauge software (Fujifilm, Tokyo, Japan).

NOX Activity Assay

NOX activity was measured by a luminescence assay in a cuvette containing 50 mmol/L phosphate buffer (pH 7.0), 1 mmol/L ethylene glycol tetraacetic acid, 150 mmol/L sucrose, 500 μmol/L lucigenin as the electron acceptor and 100 μmol/L NADPH as the substrate (total volume 900 μL) as previously described[22]. No activity was measured in the absence of NADPH. In some experiments, PP2 (final concentration 10 μmol/L) was added to the cuvette 10 min before readings. The reaction was started by the addition of 100 μL of membrane fraction (50–300 μg protein). Photon emission was measured every 15 s for 15 min in a luminometer (GloMax 20/20n

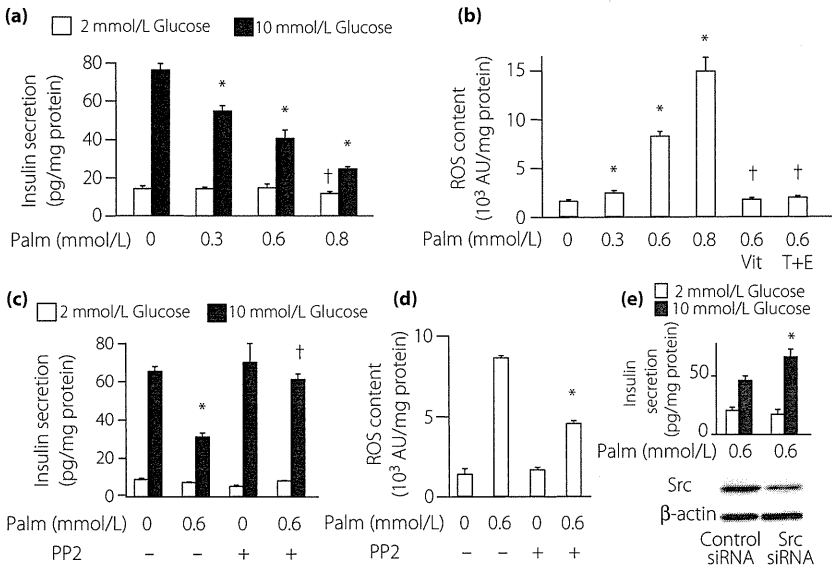

Figure 1 | Effect of palmitate exposure on glucose-induced insulin secretion (GIIS) and reactive oxygen species (ROS) production in INS-1D cells. Values are mean ± standard error of the mean (n = 4 in each bar). After INS-1D cells were cultured with or without various concentrations of palmitate (Palm) for 24 h, GIIS and ROS production were measured. (a) Effect of palmitate exposure on GIIS. GIIS was examined in the presence of 2 mmol/L (white bar) and 10 mmol/L glucose (black bar) for 30 min (n = 4 in each bar). *P < 0.01 vs 10 mmol/L glucose, culture without palmitate; †P < 0.01 vs 2 mmol/L glucose, culture without palmitate. (b) Effect of palmitate exposure on ROS production. After INS-1D cells were incubated in medium containing 2 mmol/L glucose and 10 μmol/L CM-H_2DCFDA for 60 min, ROS production was measured. ROS production was also measured using INS-1D cells cultured with 0.6 mmol/L palmitate plus ROS scavengers (0.1 mmol/L vitamin E + 0.2 mmol/L vitamin C [Vit]) or anti-oxidant mimics (10 mmol/L tempol [superoxide dismutase mimic] + 10 μmol/L ebselen [glutathione peroxidase mimic] [T + E]) for 24 h. Culturing with these agents suppressed enhanced ROS production by exposure to 0.6 mmol/L palmitate (n = 5 in each bar). *P < 0.01 vs culture without palmitate; †P < 0.01 vs culture with 0.6 mmol/L palmitate. (c) Effect of Src inhibitor on impaired GIIS by 0.6 mmol/L palmitate exposure. GIIS was measured in the presence of 2 mmol/L (white bar) and 10 mmol/L glucose (black bar) with or without 10 μmol/L 4-amino-5-(4-chlorophenyl)-7-(t-butyl)pyrazolo[3,4-d]pyrimidine (PP2) for 30 min (n = 4 in each bar). *P < 0.01 vs 10 mmol/L glucose without PP2, culture without palmitate; †P < 0.01 vs 10 mmol/L glucose without PP2, culture with 0.6 mmol/L palmitate. (d) Effect of Src inhibitor on augmented ROS production by 0.6 mmol/L palmitate exposure. After INS-1D cells were incubated in medium containing 2 mmol/L glucose and 10 μmol/L CM-H_2DCFDA with or without 10 μmol/L PP2 for 60 min, ROS production was measured (n = 5 in each bar). *P < 0.01 vs without PP2, culture with 0.6 mmol/L palmitate. (e) Effect of *Src* small interfering ribonucleic acid (siRNA) on protein expression and GIIS in INS-1D cells cultured with palmitate. After INS-1D cells transfected with control and *Src* siRNA were cultured with 0.6 mmol/L palmitate for 24 h, protein levels and GIIS were measured. Representative immunoblots were presented.

© 2013 The Authors. Journal of Diabetes Investigation published by AASD and Wiley Publishing Asia Pty Ltd

Luminometer; Promega, Fitchburg, WI, USA), which was corrected by a subtracting blank.

Small Interfering RNA Transfection

Stealth™ small interfering (si)RNAs were synthesized by Invitrogen. The sequences of siRNAs specific for rat *NCF1* (*p47^{phox}*) were as follows: 5′-GGU GAA GCC AUC GAG GUC AUU CAU A-3′, 5′-UAU GAA UGA CCU CGA UGG CUU CAC C-3′. The sequences of siRNAs specific for rat Src were as follows: 5′-GGG AGC GGC UGC AGA UUG UCA AUA A-3′, 5′-UUA UUG ACA AUC UGC AGC CGC UCC C-3′. The sequences of control siRNAs were as follows: 5′-ACC AAC AAC AGU UUG GGA AUA GGG A-3′, 5′-U CCC UAU UCC CAA ACU GUU GUU GGU -3′. Cultured INS-1D cells were trypsinized, suspended with RPMI 1640 medium without antibiotics, mixed with Opti-MEM (Invitrogen) containing siRNA and Lipofectamine 2000 (Invitrogen), plated on dishes or wells and then incubated at 37°C. The final contents of INS-1D cell, RPMI 1640, Opti-MEM, siRNA and Lipofectamine 2000 were 1 × 106 cells/mL, 75% v/v, 25% v/v, 80 nmol/L and 0.3% v/v, respectively. The medium was changed to RPMI 1640 3–4 h after transfection. All experiments using siRNA-transfected INS-1D cells were carried out 72 h after transfection.

Statistical Analysis

The data are expressed as mean ± standard error of the mean. Statistical significance was calculated by the unpaired Student's *t*-test. $P < 0.05$ was considered significant.

RESULTS

Src Inhibition Recovers Impaired Glucose-Induced Insulin Secretion and Decreases Augmented ROS Production as a Result of Exposure to Palmitate

Exposure to palmitate (C16:0) concentration dependently decreased GIIS and increased ROS production (Figure 1a,b). Oleic acid (C18:1) slightly increased ROS production, but arachidonic acid (C20:4 n-6) did not increase ROS production

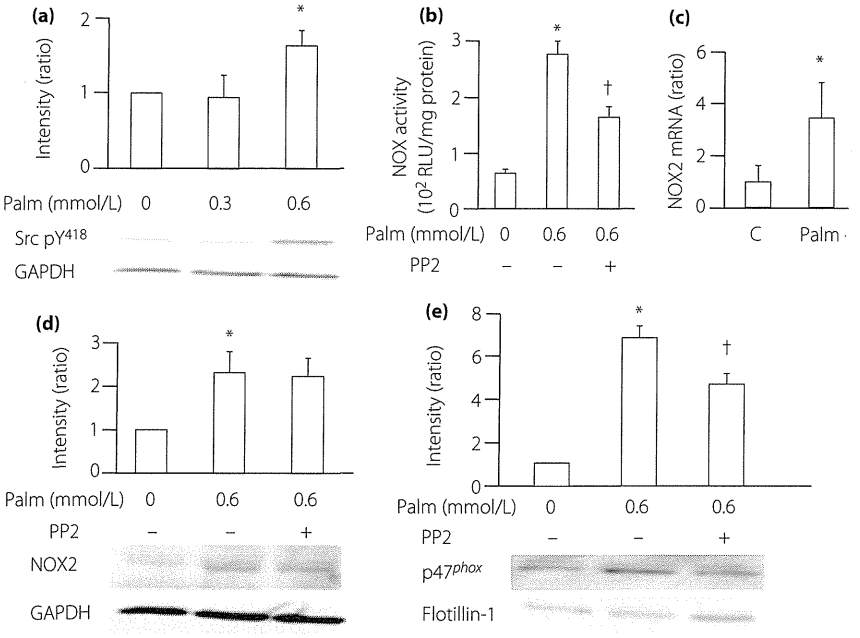

Figure 2 | Effect of palmitate exposure on Src and nicotinamide adenine dinucleotide phosphate oxidase (NOX). Values are mean ± standard error of the mean. After INS-1D cells were cultured with or without palmitate (Palm) for 24 h, and incubated with Krebs–Ringer bicarbonate HEPES with or without 10 μmol/L 4-amino-5-(4-chlorophenyl)-7-(t-butyl)pyrazolo[3,4-d]pyrimidine (PP2) for 30 min, messenger ribonucleic acid (mRNA), protein levels and NOX activity were measured. Immunoblot was carried out using (a,d) whole cell and (e) membrane fraction. (a,d,e) Representative immunoblots are presented. *$P < 0.01$ vs cultured without palmitate; †$P < 0.01$ vs without PP2, culture with 0.6 mmol/L palmitate. (a) Effect of palmitate exposure on Src activation. Src activation was detected by Tyr^{418}-phosphorylated Src. Data are expressed relative to control values without palmitate corrected by glyceraldehyde 3-phosphate dehydrogenase (GAPDH) level ($n = 5$ in each bar). (b) Effect of palmitate exposure on NOX activity. NOX activity was measured using membrane fraction ($n = 5$ in each bar). (c) Effect of palmiate exposure on expression of *NOX2/gp91^{phox}* mRNA. Data were normalized by the expression of *β-actin* ($n = 4$ in each bar). C, control without palmitate; Palm, 0.6 mmol/L palmitate. (d) Effect of palmiate exposure on expression of NOX2/gp91^{phox} protein. Data are expressed relative to control values without palmitate corrected by GAPDH level ($n = 5$ in each bar). (e) Effect of palmiate exposure on the level of p47^{phox} protein. Data are expressed relative to control values without palmitate corrected by flotillin-1 level ($n = 4$ in each bar).

© 2013 The Authors. Journal of Diabetes Investigation published by AASD and Wiley Publishing Asia Pty Ltd

(Figure S1). Exposure to 10 μmol/L PP2 for 30 min recovered impaired GIIS caused by exposure to 0.6 mmol/L palmitate for 24 h (palmitate exposure), but did not affect GIIS in the control condition without palmitate exposure (Figure 1c). Increased ROS production by palmitate exposure was reduced by 60-min exposure to 10 μmol/L PP2 (Figure 1d). Src downregulation ameliorated glucose-induced insulin secretion of INS-1D cells cultured with palmitate (Figure 1e).

Palmitate Exposure Causes NOX2 Activation by Src Activation

Palmitate exposure caused Src activation, shown by an increased protein level of Tyr^{418}-phosphorylated Src (Figure 2a). NOX activity was prominently increased by palmitate exposure (Figure 2b). Palmitate exposure also increased the messenger RNA level and protein level of NOX2 (Figure 2c,d). Exposure to 10 μmol/L PP2 for 30 min reduced augmented ROS production (Figure 2b), but did not affect the protein level of NOX2 (Figure 2d). Palmitate exposure caused an increase in the protein level of $p47^{phox}$ in membrane fraction that was reduced by exposure to PP2 for 30 min (Figure 2e). Palmitate exposure caused a decrease in the protein level of $p47^{phox}$ in cytosol fraction that was increased by exposure to PP2 for 30 min (Figure S2).

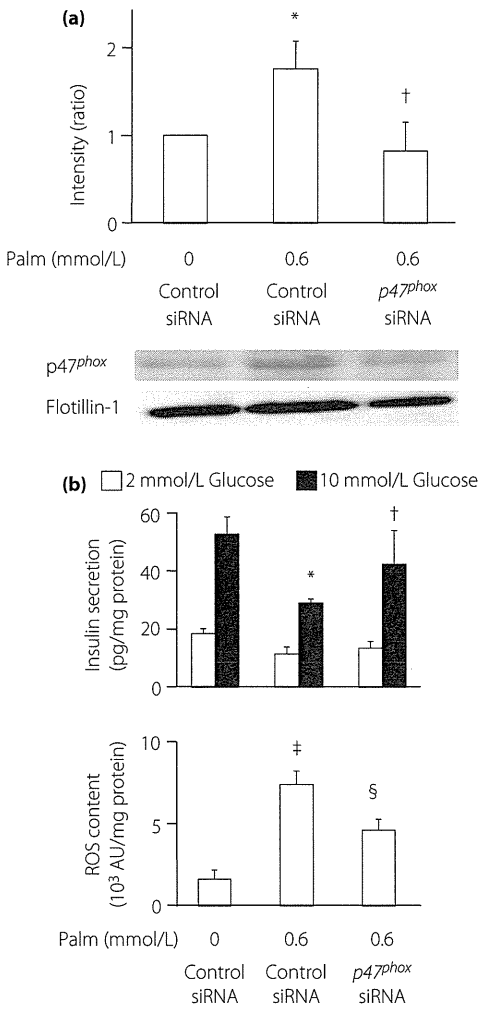

$p47^{phox}$ Knockdown Ameliorates Impaired Insulin Secretion and ROS Overproduction by Palmitate Exposure

The increased protein level of $p47^{phox}$ in membrane fraction by palmiate exposure was reduced by transfection with $p47^{phox}$ siRNA (Figure 3a). Downregulation of the $p47^{phox}$ level was also observed without palmitate exposure by $p47^{phox}$ knockdown (Figure S3). $p47^{phox}$ Knockdown ameliorated impaired GIIS, and decreased augmented ROS production by palmitate exposure (Figure 3b).

Src Inhibition Ameliorates Glucose-Induced Insulin Secretion and Decreases ROS Production in Isolated Islets of KK-A^y Mice

Impairment of GIIS from islets of KK-A^y mice was ameliorated by exposure to PP2 for 30 min (Figure 4a). ROS production and the level of $p47^{phox}$ protein in membrane fraction in the islets of KK-A^y mice was reduced by exposure to PP2 (Figure 4b,c). The protein level of Tyr^{418}-phosphorylated Src was increased in KK-A^y mice islets compared with that in control islets (Figure S4).

DISCUSSION

Exposure to palmitate, a saturated non-esterified fatty acid decreased GIIS and increased ROS production (Figure 1a,b), as

Figure 3 | Effect of $p47^{phox}$ siRNA on protein expression, glucose-induced insulin secretion (GIIS) and reactive oxygen species (ROS) production. Values are mean ± standard error of the mean. After INS-1D cells transfected with control and $p47^{phox}$ small interfering ribonucleic acid (siRNA) were cultured with or without 0.6 mmol/L palmitate (Palm) for 24 h, protein levels, GIIS and ROS production were measured. (a) Effect of $p47^{phox}$ knockdown on enhanced expression of $p47^{phox}$ protein by palmitate exposure. Immunoblot was carried out using membrane fraction. Data are expressed relative to control values transfected with control siRNA and cultured without palmitate corrected by flotillin-1 level (n = 5 in each bar). *P < 0.01 vs transfected with control siRNA, cultured without palmitate; †P < 0.01 vs control siRNA transfected, cultured with 0.6 mmol/L palmitate. Representative immunoblots are presented. (b) Effect of $p47^{phox}$ knockdown on impaired GIIS (upper panel) and increased ROS production (lower panel) by palmitate exposure. Upper panel: GIIS was examined in the presence of 2 mmol/L (white bar) and 10 mmol/L glucose (black bar) for 30 min (n = 4 in each bar). *P < 0.01 vs transfected with control siRNA, culture without palmitate, 10 mmol/L glucose. †P < 0.01 vs transfected with control siRNA, culture with 0.6 mmol/L palmitate, 10 mmol/L glucose. Lower panel: After cells were incubated in medium containing 2 mmol/L glucose and 10 μmol/L CM-H_2DCFDA for 60 min, ROS production was measured (n = 5 in each bar). ‡P < 0.01 vs transfected with control siRNA, cultured without palmitate. §P < 0.01 vs control siRNA transfected, cultured with 0.6 mmol/L palmitate.

© 2013 The Authors. Journal of Diabetes Investigation published by AASD and Wiley Publishing Asia Pty Ltd

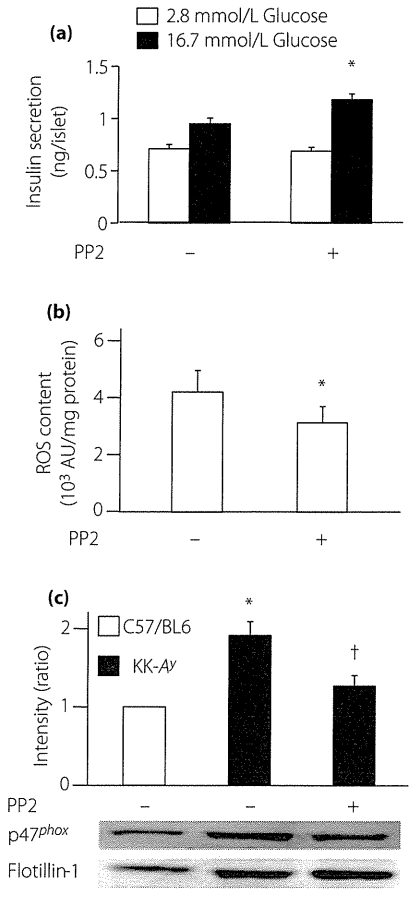

Figure 4 | Effect of Src inhibition on glucose-induced insulin secretion (GIIS) and reactive oxygen species (ROS) production, and the protein level of $p47^{phox}$ in KK-A^y mouse islets. Values are mean ± standard error of the mean. (a) Effect of Src inhibition on GIIS. Freshly isolated islets of KK-A^y mice were batch-incubated in the presence of 2.8 mmol/L (white bar) and 16.7 mmol/L glucose (black bar) with or without 10 μmol/L 4-amino-5-(4-chlorophenyl)-7-(t-butyl)pyrazolo[3,4-d] pyrimidine (PP2) for 30 min, and released insulin in the medium was measured (n = 5 in each bar). *P < 0.01 vs without PP2, 16.7 mmol/L glucose. (b) Effect of Src inhibition on ROS production. Freshly isolated islets of KK-A^y mice were batch-incubated in the presence of 2.8 mmol/L with or without 10 μmol/L PP2 for 60 min, and ROS production was measured (n = 3 in each bar). *P < 0.05 vs without PP2. (c) Effect of cSrc inhibition on the protein level of $p47^{phox}$. Freshly isolated islets of control C57/BL6 mice (white bar) and KK-A^y mice (black bar) were batch-incubated in the presence of 2.8 mmol/L with or without 10 μmol/L PP2 for 30 min, and the protein level of $p47^{phox}$ was measured using membrane fraction (n = 4 in each bar). Data are expressed relative to control values of C57/BL6 mice corrected by flotillin-1 level. *P < 0.01 vs C57/BL6. †P < 0.01 vs KK-A^y without PP2. Representative immunoblots are presented.

previously described[8,9]. We have previously described an important role of endogenous ROS production that involves Src activation in impaired GIIS in diabetic islets[13–15]. In the present study, we investigated the effects of PP2, a specific Src inhibitor, on impaired GIIS and augmented ROS production by lipotoxicity. Exposure to PP2 ameliorated impaired GIIS and decreased augmented ROS production by palmitate exposure (Figure 1c,d). In addition, Src downregulation ameliorated impairment of GIIS by palmitate exposure (Figure 1e). These results suggest that Src activation might be involved in impaired GIIS and augmented ROS production as a result of palmitate exposure.

Src is a non-receptor tyrosine kinase that is associated with the cell membrane and plays important roles in various signal transductions. Its activity is regulated by intramolecular interactions that depend on tyrosine phosphorylation and phosphorylation of Tyr^{418} at the kinase domain that results in Src activation[23]. Palmitate exposure caused Src activation indicated by an increased protein level of Tyr^{418}-phosphorylated Src (Figure 2a). In a recent study, it was proposed that palmitate alters membrane distribution of Src, causing it to partition into intracellular membrane subdomains, where it likely becomes autophosphorylated and activated[24]. NOX2 ($gp91^{phox}$ and $p22^{phox}$), an isoform of NOX, and its related subunits ($p47^{phox}$ and $p67^{phox}$) are expressed in β-cells[11,12,25–27]. Interestingly, exposure to palmitate affects expression level of $p47^{phox}$ in islets[10]. In addition, impaired GIIS and an increase in apoptosis by chronic exposure to palmitate are restored by suppression of NOX2 with a decrease in ROS level in a β-cell line[9]. The effects of palmitate exposure on NOX2 and involvement of Src were therefore examined. NOX activity was prominently increased by palmitate exposure (Figure 2b). PP2 reduced augmented ROS production (Figure 2b), but did not affect protein level of NOX2 (Figure 2d). These results suggest that Src activation might affect regulatory factor(s) of NOX. An important role of Src in activation of NOX2 through translocation of $p47^{phox}$ to plasma membrane has been reported in various cells[16,17]. In addition, cigarette smoke particle-phase extract induces Src activation, which causes NOX2, Src and $p47^{phox}$ complex formation that increases NOX activity in smooth muscle cells[28]. Palmitate exposure was found to cause an increase in protein level of $p47^{phox}$ in membrane fraction that was reduced by PP2 (Figure 2e). Taken together, these findings show that palmitate exposure increases NOX activity mainly by increasing translocation of $p47^{phox}$ to plasma membrane through Src signaling.

To elucidate the role of $p47^{phox}$ in impaired insulin secretion and ROS overproduction by palmitate exposure, the effect of *$p47^{phox}$* knockdown on GIIS and ROS production was examined. *$p47^{phox}$* Knockdown ameliorated impaired GIIS and decreased augmented ROS production by palmitate exposure (Figure 3B). These results show that $p47^{phox}$ is involved in impaired GIIS and ROS overproduction by palmitate exposure.

Src inhibition by PP2 treatment completely recovered palmitate-induced GIIS impairment despite partial reduction of NOX activation and $p47^{phox}$ expression in the membrane in INS-1D cells. Explanation of these findings is difficult using the data in the present study, but one possibility is that palmitate exposure

© 2013 The Authors. Journal of Diabetes Investigation published by AASD and Wiley Publishing Asia Pty Ltd

also decreases vulnerability to ROS in β-cell function. In addition, it is proposed that Src is constantly activated by forming an intracellular disulphide bond derived from ROS exposure[29], which could affect the concentration-dependent effect of Src inhibitors. Suppression of ROS content was partial despite complete suppression of the $p47^{phox}$ level by knockdown. These phenomena might be explained by the fact that palmitate exposure increases NOX2 expression in addition to the $p47^{phox}$ level (Figure 2c,d).

NOX2 expression is upregulated in islets from obese diabetic mice[11,12] and rats[11]. The pathophysiological significance of the results in the present study was examined using isolated islets of KK-A^y mice, an obese diabetic model with hyperlipidemia. Impairment of GIIS from islets of KK-A^y mice was ameliorated by PP2 (Figure 4a). In addition, ROS production and the level of $p47^{phox}$ protein in membrane fraction in the islets of KK-A^y mice was reduced by exposure to PP2 (Figure 4b,c). These results suggest that activation of NOX through Src signaling might be involved in impairment of GIIS from islets of KK-A^y mice.

The ameliorating effect of Src inhibition on GIIS is less in islets of obese KK-A^y mice than it is in islets of non-obese GK rats[13]. As shown in Figure S4, Src activation is similar in KK-A^y mice islets to that in GK rat islets[14]. This indicates that the differing effect of Src inhibition on GIIS is not derived from the different level of Src activation. Impairment of GIIS is more prominent in KK-A^y mice islets than in GK rat islets. Another mechanism of impaired GIIS independent of ROS overproduction might exist in obese mice islets. Severe impairment of GIIS is also observed in islets of *ob/ob* mice, another obese diabetic model, in which upregulation of UCP-2 derived from upregulation of TBP-2 plays an important role in impaired GIIS[19]. In contrast, we observed neither UCP-2 upregulation nor TBP-2 upregulation in GK rat islets (unpublished observation).

In conclusion, activation of NOX through Src signaling plays an important role in ROS overproduction and impaired GIIS caused by chronic exposure to palmitate, suggesting a lipotoxic mechanism of β-cell dysfunction in obese mice.

ACKNOWLEDGEMENTS

The authors have nothing to disclose. The present study was supported by a Research Grant on Nanotechnical Medicine from the Ministry of Health, Labor and Welfare of Japan; Scientific Research Grants from the Ministry of Education, Culture, Sports, Science and Technology of Japan; and a grant from CREST of the Japan Science and Technology Cooperation. We thank C Kotake and M Akazawa for technical assistance.

REFERENCES

1. Meglasson MD, Matschinsky FM. Pancreatic islet glucose metabolism and regulation of insulin secretion. *Diabetes Metab Rev* 1986; 2: 163–214.
2. Krippeit-Drews P, Kramer C, Welker S, *et al.* Interference of H_2O_2 with stimulus-secretion coupling in mouse pancreatic β-cells. *J Physiol* 1999; 514: 471–481.
3. Maechler P, Jornot L, Wollheim CB. Hydrogen peroxide alters mitochondrial activation and insulin secretion in pancreatic beta cells. *J Biol Chem* 1999; 274: 27905–27913.
4. Bindokas VP, Kuznetsov A, Sreenan S, *et al.* Visualizing superoxide production in normal and diabetic rat islets of Langerhans. *J Biol Chem* 2003; 278: 9796–9801.
5. Turrens JF. Mitochondrial formation of reactive oxygen species. *J Physiol* 2003; 552: 335–344.
6. Guichard C, Moreau R, Pessayre D, *et al.* NOX family NADPH oxidases in liver and in pancreatic islets: a role in the metabolic syndrome and diabetes? *Biochem Soc Trans* 2008; 36: 920–929.
7. Poitout V, Robertson RP. Minireview: Secondary β-cell failure in type 2 diabetes-a convergence of glucotoxicity and lipotoxicity. *Endocrinology* 2002; 143: 339–242.
8. Carlsson C, Borg LA, Welsh N. Sodium palmitate induces partial mitochondrial uncoupling and reactive oxygen species in rat pancreatic islets *in vitro*. *Endocrinology* 1999; 140: 3422–3428.
9. Yuan H, Zhang X, Huang X, *et al.* NADPH oxidase 2-derived reactive oxygen species mediate FFAs-induced dysfunction and apoptosis of β-cells via JNK, p38 MAPK and p53 pathways. *PLoS ONE* 2010; 5: e15726.
10. Morgan D, Oliveira-Emilio HR, Keane D, *et al.* Glucose, palmitate and pro-inflammatory cytokines modulate production and activity of a phagocyte-like NADPH oxidase in rat pancreatic islets and a clonal beta cell line. *Diabetologia* 2007; 50: 359–369.
11. Nakayama M, Inoguchi T, Sonta T, *et al.* Increased expression of NAD(P)H oxidase in islets of animal models of type 2 diabetes and its improvement by an AT1 receptor antagonist. *Biochem Biophys Res Commun* 2005; 332: 927–933.
12. Shao J, Iwashita N, Ikeda F, *et al.* Beneficial effects of candesartan, an angiotensin II type 1 receptor blocker, on beta-cell function and morphology in db/db mice. *Biochem Biophys Res Commun* 2006; 344: 1224–1233.
13. Kominato R, Fujimoto S, Mukai E, *et al.* Src activation generates reactive oxygen species and impairs metabolism-secretion coupling in diabetic Goto-Kakizaki and ouabain-treated rat pancreatic islets. *Diabetologia* 2008; 51: 1226–1235.
14. Mukai E, Fujimoto S, Sato H, *et al.* Exendin-4 suppresses Src activation and reactive oxygen species production in diabetic Goto-Kakizaki rat islets in an Epac-dependent manner. *Diabetes* 2011; 60: 218–226.
15. Kajikawa M, Fujimoto S, Tsuura Y, *et al.* Ouabain suppresses glucose-induced mitochondrial ATP production and insulin release by generating reactive oxygen species in pancreatic islets. *Diabetes* 2002; 51: 2522–2529.

© 2013 The Authors. Journal of Diabetes Investigation published by AASD and Wiley Publishing Asia Pty Ltd

16. Chowdhury AK, Watkins T, Parinandi NL, *et al.* Src-mediated tyrosine phosphorylation of $p47^{phox}$ in hyperoxia-induced activation of NADPH oxidase and generation of reactive oxygen species in lung endothelial cells. *J Biol Chem* 2005; 280: 20700–20711.
17. Lin CC, Lee IT, Yang YL, *et al.* Induction of COX-2/PGE(2)/IL-6 is crucial for cigarette smoke extract-induced airway inflammation: role of TLR4-dependent NADPH oxidase activation. *Free Radic Biol Med* 2010; 48: 240–254.
18. Nishi Y, Fujimoto S, Sasaki M, *et al.* Role of mitochondrial phosphate carrier in metabolism-secretion coupling in rat insulinoma cell line INS-1. *Biochem J* 2011; 435: 421–430.
19. Yoshihara E, Fujimoto S, Inagaki N, *et al.* Disruption of TBP-2/Txnip ameliorates insulin sensitivity and secretion without affecting obesity. *Nat Commun* 2010; 1: article number 127.
20. Lacraz G, Figeac F, Movassat J, *et al.* Diabetic β-cells can achieve self-protection against oxidative stress through an adaptive up-regulation of their antioxidant defenses. *PLoS ONE* 2009; 4: e6500.
21. Zhao LX, Zhou CJ, Tanaka A, *et al.* Cloning, characterization and tissue distribution of the rat ATP-binding cassette (ABC) transporter ABC2/ABCA2. *Biochem J* 2000; 350: 865–872.
22. Zafari AM, Ushio-Fukai M, Akers M, *et al.* Role of NADH/NADPH oxidase-derived H_2O_2 in angiotensin II-induced vascular hypertrophy. *Hypertension* 1998; 32: 488–495.
23. Martin GS. The hunting of the Src. *Nat Rev Mol Cell Biol* 2001; 2: 467–475.
24. Holzer RG, Park EJ, Li N, *et al.* Saturated fatty acids induce c-Src clustering within membrane subdomains, leading to JNK activation. *Cell* 2011; 147: 173–184.
25. Oliveira HR, Verlengia R, Carvalho CR, *et al.* Pancreatic β-cells express phagocyte-like NAD(P)H oxidase. *Diabetes* 2003; 52: 1457–1463.
26. Lupi R, Del Guerra S, Bugliani M, *et al.* The direct effects of the angiotensin-converting enzyme inhibitors, zofenoprilat and enalaprilat, on isolated human pancreatic islets. *Eur J Endocrinol* 2006; 154: 355–361.
27. Uchizono Y, Takeya R, Iwase M, *et al.* Expression of isoforms of NADPH oxidase components in rat pancreatic islets. *Life Sci* 2006; 80: 133–139.
28. Cheng SE, Lee IT, Lin CC, *et al.* Cigarette smoke particle-phase extract induces HO-1 expression in human tracheal smooth muscle cells: role of the c-Src/NADPH oxidase/MAPK/Nrf2 signaling pathway. *Free Radic Biol Med* 2010; 48: 1410–1422.
29. Giannoni E, Taddei ML, Chiarugi P. Src redox regulation: again in the front line. *Free Radic Biol Med* 2010; 49: 516–527.

SUPPORTING INFORMATION

Additional Supporting Information may be found in the online version of this article:

Figure S1 | Effect of oleic acid (Ole) and arachidonic acid (Ara) exposure on reactive oxygen species (ROS). After INS-1D cells were cultured with 0.1 mmol/L palmitate, 0.6 mmol/L palmitate, 0.1 mmol/L Ole and 0.1 mmol/L Ara for 24 h, ROS production was measured. Values are mean ± standard error of the mean; $n = 4$ in each bar. $^*P < 0.01$ vs control without free fatty acid.

Figure S2 | Representative immunoblots of $p47^{phox}$ in the cytosol fraction from two independent experiments. After INS-1D cells were cultured with or without palmitate (Palm) for 24 h and incubated with Krebs–Ringer bicarbonate HEPES with or without 10 μmol/L 4-amino-5-(4-chlorophenyl)-7-(t-butyl)pyrazolo[3,4-d]pyrimidine (PP2) for 30 min, immunoblots of the cytosol fraction were carried out.

Figure S3 | Effect of *$p47^{phox}$* small interfering ribonucleic acid (siRNA) on basal $p47^{phox}$ level in membrane fraction without palmitate exposure. After INS-1D cells transfected with control, and *$p47^{phox}$* siRNA were cultured without palmitate for 24 h, protein levels were measured. Immunoblot was carried out using membrane fraction. Data are expressed relative to control values transfected with control siRNA corrected by flotillin-1 level. Values are mean ± standard error of the mean. $^*P < 0.01$ vs transfected with control siRNA; $n = 3$ in each bar.

Figure S4 | Representative immunoblots of Src in islets of KK-A^y mice and control C57/BL6 mice from two independent experiments. Src activation was detected by Tyr^{418}-phosphorylated Src. The numbers of the side of each panel express the ratio to value of control islets.

© 2013 The Authors. Journal of Diabetes Investigation published by AASD and Wiley Publishing Asia Pty Ltd

Diabetologia (2013) 56:2609–2618
DOI 10.1007/s00125-013-3031-9

ARTICLE

Mutations in *KCNJ11* are associated with the development of autosomal dominant, early-onset type 2 diabetes

Limei Liu · Kazuaki Nagashima · Takao Yasuda · Yanjun Liu · Hai-rong Hu · Guang He · Bo Feng · Mingming Zhao · Langen Zhuang · Taishan Zheng · Theodore C. Friedman · Kunsan Xiang

Received: 1 June 2013 / Accepted: 2 August 2013 / Published online: 10 September 2013
© Springer-Verlag Berlin Heidelberg 2013

Abstract

Aims/hypothesis More than 90% of Chinese familial early-onset type 2 diabetes mellitus is genetically unexplained. To investigate the molecular aetiology, we identified and characterised whether mutations in the *KCNJ11* gene are responsible for these families.

Methods *KCNJ11* mutations were screened for 96 familial early-onset type 2 diabetic probands and their families. Functional significance of the identified mutations was confirmed by physiological analysis, molecular modelling and population survey.

Results Three novel *KCNJ11* mutations, R27H, R192H and S116F117del, were identified in three families with early-onset type 2 diabetes mellitus. Mutated *KCNJ11* with R27H or R192H markedly reduced ATP sensitivity (E23K>R27H>C42R>R192H>R201H), but no ATP-sensitive potassium channel currents were detected in the loss-of-function S116F117del channel in vitro. Molecular modelling indicated that R192H had a larger effect on the channel ATP-binding pocket than R27H, which may qualitatively explain why the ATP sensitivity of the R192H mutation is seven times less than R27H. The shape of the S116F117del channel may be compressed, which may explain why the mutated channel had no currents. Discontinuation of insulin and implementation of sulfonylureas for R27H or R192H carriers and continuation/switch to insulin therapy for S116F117del carriers resulted in good glycaemic control.

Conclusions/interpretation Our results suggest that genetic diagnosis for the *KCNJ11* mutations in familial early-onset type 2 diabetes mellitus may help in understanding the molecular aetiology and in providing more personalised treatment for these specific forms of diabetes in Chinese and other Asian patients.

Keywords Familial early-onset type 2 diabetes mellitus · *KCNJ11* · Kir6.2 · Mutation

Abbreviations

HI	Hyperinsulinism
IA-2	Tyrosine phosphatase-like protein
IGT	Impaired glucose tolerance
K_{ATP}	ATP-sensitive potassium channel
MODY	Maturity-onset diabetes of the young

Limei Liu, Kazuaki Nagashima, Takao Yasuda, Yanjun Liu, Hai-rong Hu and Guang He contributed equally to this study.

L. Liu (✉) · M. Zhao · L. Zhuang · T. Zheng · K. Xiang
Department of Endocrinology & Metabolism, Shanghai Jiaotong University Affiliated Sixth People's Hospital, Shanghai Diabetes Institute, 600 Yishan Road, Shanghai 200233, China
e-mail: lmliu@sjtu.edu.cn

K. Nagashima
Department of Diabetes and Clinical Nutrition, Graduate School of Medicine, Kyoto University, Kyoto, Japan

T. Yasuda
Division of Cellular and Molecular Medicine, Department of Physiology and Cell Biology, Kobe University Graduate School of Medicine, Kobe, Japan

Y. Liu · T. C. Friedman
UCLA School of Medicine, Division of Endocrinology, Charles R. Drew University of Medicine & Sciences, Los Angeles, CA, USA

H.-r. Hu
State Key Laboratory of Genetic Engineering, School of Life Sciences, Fudan University, Shanghai, China

G. He
Bio-X Center, Key Laboratory for the Genetics of Developmental and Neuropsychiatric Disorders (Ministry of Education), Shanghai Jiaotong University, Shanghai, China

B. Feng
Department of Endocrinology, Tongji University, The Affiliated East Hospital, Tongji University, Shanghai, China

PNDM	Permanent neonatal diabetes
SNP	Single nucleotide polymorphism
TM	Transmembrane

Introduction

Maturity-onset diabetes of the young (MODY) is a monogenic, autosomal dominant, early-onset form of non-autoimmune diabetes caused by primary pancreatic beta cell dysfunction [1], and more than ten MODY genes have been identified [2, 3]. The clinical phenotype of familial early-onset type 2 diabetes mellitus is often characterised by insulin resistance, in contrast with MODY, which is similar to later-onset type 2 diabetes [4]. Heterozygous activating mutations in *KCNJ11* have been reported as a cause of not only permanent neonatal diabetes (PNDM) [2, 5] but also MODY and adult-onset diabetes in a number of studies [6]. This was reaffirmed in a French MODY gene-negative pedigree last year [7], wherein the defined *KCNJ11* gene was proposed to be MODY13.

KCNJ11 on 11p15.1 is a single open reading frame encoding a 390-amino acid protein, potassium inwardly-rectifying channel Kir6.2, which contains two putative transmembrane (TM) segments and a pore loop domain, H5 (Fig. 1a) [8, 9]. ATP-sensitive potassium channels (K_{ATP}) control electrical signalling by coupling cellular metabolism to potassium ion movement across cell membranes. Pancreatic beta cell K_{ATP} channels comprise two components: four subunits of Kir6.2 forming the channel pore, and the sulfonylurea receptor, SUR1, regulating channel gating [10]. The K_{ATP} channel is sensitive to ATP and inhibited by sulfonylureas [11], drugs that are widely used to treat type 2 diabetes and regulate insulin secretion by coupling the metabolic state of the cell to membrane potential.

Mutations (e.g. E227K) [7] and variations (e.g. E23K) [12] in *KCNJ11* have already been linked to diabetes. In Kir6.2 knockout mice, both glucose- and tolbutamide-induced insulin secretion and membrane depolarisation and calcium influx into beta cells are defective, indicating that the regulation of insulin secretion depends on K_{ATP} channel activity [13]. A high frequency of beta cell apoptosis is observed in Kir6.2G132S transgenic mice before the appearance of hyperglycaemia, suggesting that K_{ATP} channels also play a significant role in beta cell survival [14].

We screened a cohort of 96 MODY gene-negative probands with early-onset autosomal dominant type 2 diabetes, and their families, for *KCNJ11* mutations, and report here three novel heterozygous *KCNJ11* mutations associated with MODY gene-negative autosomal dominantly inherited type 2 diabetes.

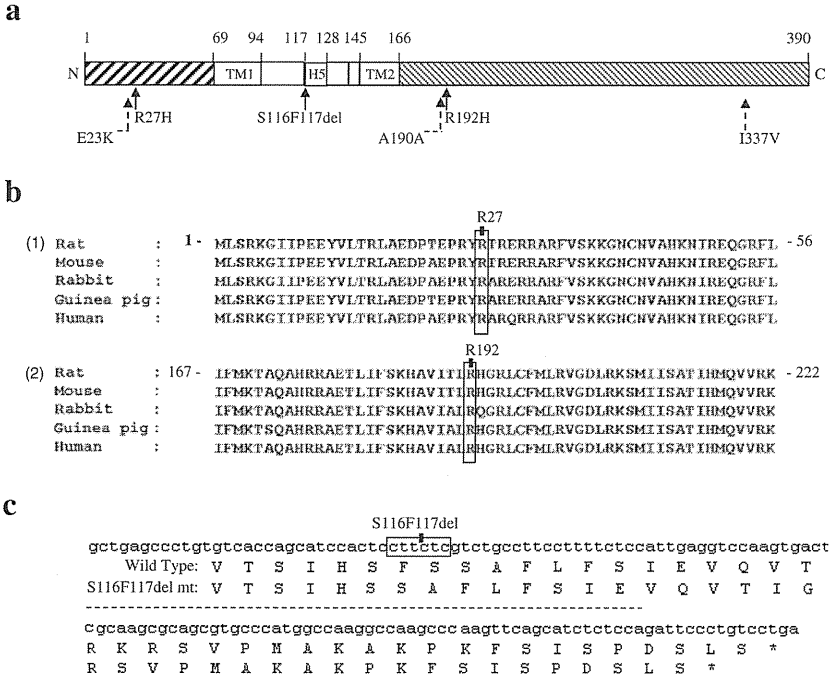

Fig. 1 Identification of *KCNJ11* mutations. (**a**) Schematic illustration of *KCNJ11* and the corresponding domains in Kir6.2. Numbers refer to the amino acids bordering the domains. Filled arrows indicate the mutations identified in *KCNJ11*. Dashed arrows indicate single-nucleotide polymorphisms (SNPs) identified in KCNJ11. The gene borders were determined based on mammalian homology using published data [8, 9]. N, N-terminus; C, C-terminus; TM1, first TM domain; H5, pore loop domain; TM2, second TM domain. (**b**) Alignment of specific regions of *KCNJ11*/Kir6.2 from different mammals using ClustalX. (1) Entire 68-amino acid N-terminal domain of *KCNJ11*/Kir6.2; the R27 residue is indicated. (2) Portion of the C-terminal domain of *KCNJ11*/Kir6.2; the R192 residue is indicated. (**c**) Fragment of the *KCNJ11*/Kir6.2 sequence; the S116F117del is indicated. The corresponding amino acid sequences of wild-type Kir6.2 and the S116F117del mutation (mt) are shown; the S116F117del results in truncated Kir6.2 lacking two amino acids (Ser116 and Phe117)

Methods

Recruitment of diabetic index cases and families We recruited the families for studies on the genetics of type 2 diabetes at the Shanghai Diabetes Institute, Shanghai Diabetic Clinical Medical Center. Briefly, families were selected if their pattern of type 2 diabetes was consistent with autosomal dominant inheritance. An additional selection criterion was the availability of a large number of family members (with and without diabetes) who agreed to participate in the study. The screening criteria for eligible families were: (1) at least one index case (early-onset type 2 diabetes diagnosed <40 years old; range 12–39 years old); (2) index case treatment by dietary control or oral agents for the first 2 years; (3) diabetes in at least three generations; (4) index cases without the mitochondrial DNA 3243 A-to-G point mutation, as confirmed by PCR–RFLP analysis, using ApaI (Promega, Madison, WI, USA), as described by Fukui et al [15] with slight modifications; (5) index cases without mutations in the following six MODY genes [16]: *HNF4α/MODY1*, *GCK/MODY2*, *HNF1α/MODY3*, *PDX1/MODY4*, *HNF1β/MODY5* and *NEUROD1/BETA2/MODY6*, confirmed by PCR-direct sequencing, as previously reported with some modifications [17–22]. No deletions of these six MODY genes were excluded by performing multiplex ligation-dependent probe amplification (MLPA) in the set of the 96 early-onset type 2 diabetic probands. To date, we have recruited and examined 96 families of Han Chinese and measured their height, weight and blood pressure, and blood was obtained for DNA extraction and biochemical measurements, including blood glucose, triacylglycerol, total cholesterol, HbA_{1c}, C-peptide and insulin. From participants without diabetes and diabetic patients treated with oral agents or diet, we took blood again 2 h after an OGTT (75 g glucose) to determine blood glucose, C-peptide and insulin. In addition, fasting serum C-peptide in insulin-treated individuals was measured.

We selected 109 non-diabetic participants according to the following criteria: over 65 years of age (age 73.2±5.7 years; BMI 21.1±2.4 kg/m^2 [means ± SD]), normal glucose tolerance, HbA_{1c}<5.6% (38 mmol/mol) and no family history of diabetes. All participants completed medical and family history questionnaires; this information was supplemented with information from medical records. The ADA criteria were used to diagnose diabetes and impaired glucose tolerance (IGT) [23].

All patients underwent a standardised clinical and laboratory evaluation. Serum antibodies against GAD and protein tyrosine phosphatase-like protein (IA-2) were tested using a radioimmunoprecipitation kit with ^{125}I-labelled GAD65 and ^{125}I-labelled IA-2, according to the manufacturer's recommendations (RSR, Cardiff, UK). The criterion for a positive assay for each antibody was an index >1.0 (2 SDs above the mean value in normal controls). Serum insulin and C-peptide were measured by an RIA (Linco Research, St Charles, MO, USA). The insulin assay showed little cross-reactivity (<2%) with human proinsulin. Triacylglycerol and total cholesterol were determined by enzymatic procedures using an autoanalyser (Hitachi 7600-020; Hitachi, Tokyo, Japan). All the patients in this study had negative results for GAD and IA-2 antibodies and 3243 A-to-G point mutation.

This study was approved by the institutional review board of Shanghai Jiaotong University Affiliated Sixth People's Hospital. Written informed consent was obtained from all participants.

Sequencing of KCNJ11 We used two pairs of primers to sequence the entire coding sequence and flanking sequences of *KCNJ11* (forward, 5′-CGAGAGGACTCTGCAGTGAG-3′, reverse, 5′-GCTTGCTGAAGATGAGGGTC-3′; and forward, 5′-CATCGTGCAGAACATCG-TG-3′, reverse, 5′-TAACACCCTGGATGAGCAG-3′) [6]. PCR was performed using each pair of specific primers at 95°C for 5 min, followed by 30 cycles of denaturation at 95°C for 1 min, annealing at 58°C for 1 min, extension at 72°C for 1 min and a final extension of 10 min on the Gene Amp PCR system 9700 thermocycler (PE Applied Biosystems, Foster City, CA, USA). Amplified DNA was purified using the QIAquick PCR Purification Kit (Qiagen, Shanghai, China) and sequenced from both ends using specific primers and the BigDye Terminator cycle sequencing kit (version 3.1; Applied Biosystems). Electrophoresis was performed on the ABI PRISM 3100 Genetic Analyzer, and ABI PRISM Sequencing Analysis software version 3.7 was used for analysis. We confirmed the sequence of the three mutations by cloning the PCR product of the entire coding sequence of the genes into a TA cloning vector (PCR 2.1; Invitrogen, Shanghai, China) and sequencing. Sequences were compared with the published sequence (NM_000525.3) using Sequence Navigator (Applied Biosystems). Novel mutations were tested for cosegregation with diabetes in other family members and the 109 normal individuals of Han Chinese origin.

Parametric linkage analysis Genotyping data were calculated using the MLINK subprogram from the LINKAGE package (version 5.1) for two-point linkage analysis. Autosomal dominant inheritance was assumed, with a disease-gene frequency of 0.0001 and 80% penetrance.

Construction of the three KCNJ11 mutants Mammalian expression plasmids containing the whole coding regions of human *KCNJ11* and *ABCC8* (also known as *SUR1*) have been described previously [6, 8]. Human *KCNJ11* cDNA was subcloned into pCMV vector (Promega, Madison, WI, USA), and a single-stranded template of pCMV *KCNJ11* was prepared using the helper phage R408. Expression plasmids with R27H, R192H or S116F117del mutations were generated by site-directed mutagenesis.

Cell culture and DNA transfection COS-1 cells were cultured in DMEM supplemented with 10% FBS. For single-channel recordings, 1×10^5 cells were plated in 35 mm dishes, and transfected with 1.5 μmol/l pCMV6c carrying wild-type *ABCC8* and 1.5 μmol/l pCMV6b carrying wild-type *KCNJ11* or mutated *KCNJ11* (R27H, R192H or S116F117del) using Lipofectamine 2000 (Invitrogen) according to the manufacturer's instructions; pEGFP-N1 (Clontech, Palo Alto, CA, USA) encoding green fluorescent protein was also cotransfected as a reporter gene [14]. The cells were cultured for 48–72 h before electrophysiological recordings.

Electrophysiology Single-channel recordings were performed using the excised inside–out membrane patch configuration, as previously described [14]. Single-channel currents were analysed using a combination of pCLAMP (version 9.0; Axon Instruments, Foster City, CA, USA) and in-house software. The ATP sensitivity of the wild-type and mutant channels was determined using an Axopatch 200B patch-clamp amplifier (Axon Instruments). Sulfonylurea sensitivity was assessed as the ratio between the amplitudes of the K_{ATP} channel currents before and after application of 100 μmol/l tolbutamide. Experiments were conducted for both the wild-type ($n=15$) and mutant (Kir6.2 R27H/SUR1, $n=10$; Kir6.2 R192H/SUR1, $n=9$) channels. The results are expressed as means ± SE; Mann–Whitney *U* tests (detectable rate of the channels) or unpaired Student's *t* tests were used to test for statistical significance.

Model building of Kir6.2 To further explore the effect of the mutations on the function of Kir6.2, we constructed a molecular model of the C-terminus of Kir6.2, based on the crystal structure of Kir2.1 [24]. The N-terminal domains of these proteins share 53.1% sequence identity. The sequences were aligned using ClustalX (Clustal X version 2.0, www.clustal.org/clustal2/). Homology models were generated using CPHmodels-2.0 Server and swiss-model. The model of Kir6.2 (residues 1-177) was based on the crystal structures of the bacterial inwardly rectifying K^+ channel (KirBac3.1; PDB entry 1U4F) and the intracellular domain of the rat Kir3.1 channel (PDB entry 1X6L). The TM region of Kir channels is highly conserved. The level of conservation between the TM regions of KirBac3.1 and rat Kir3.1 is 36%, indicating that the TM region of KirBac3.1 would be an appropriate model for the TM segment of Kir3.1. The TM region was modelled as a tetramer with fourfold symmetry imposed. The three segments of the model (TMs, N and C domains) were constructed separately and then joined together. The structure constructed is similar to a previous report [25] and is a truncated form of Kir6.2 in the absence of SUR1. However, this predicted Kir6.2 model is hypothetical and requires further verification. Homology modelling was also performed for the pore-forming inwardly rectifying potassium channel Kir6.2 subunits, to provide a rational explanation for the effects of the mutations.

Results

Genetic analysis Six *KCNJ11* variants were identified in the MODY gene-negative families: three known single-nucleotide polymorphisms (SNPs) (E23K [rs5219], A190A [rs5218] and I337V [rs5215]) and three novel mutations (c.80G>A, p.R27H; c.575G>A, p.R192H; and c.348-353delCTTCTC, p.S116F117del) (Fig. 1a). The frequencies of the three SNPs (E23K [rs5219], A190A [rs5218] and I337V [rs5215]) were similar in the 96 index cases and 109 unrelated non-diabetic individuals (39.1% vs 38.5%, 43.7% vs 46.8% and 40.0% vs 38.5%, respectively). The three novel mutations (R27H, R192H and S116F117del) were detected in three individual index cases, but not in the other probands or 109 non-diabetic controls, suggesting that these mutations are not simple polymorphisms.

Bioinformatics and functional analysis of mutant channels The index case from family a had an amino acid substitution in codon 27 (NM_000525.3: c.80G>A, p.R27H) (Fig. 1b). R27H is located in the cytosolic region of the N-terminal domain close to the ATP-binding sites (R201 and K185) in the C-terminus of a single subunit of Kir6.2 in steric conformation (Fig. 2). As Arg is positively charged, R27H may reduce the ligand-binding affinity of Kir6.2, by reducing positive charge distribution and increasing steric repulsion between two adjacent ATP-binding pocket monomers.

The index case from family b had an amino acid substitution in codon 192 (NM_000525.3: c.575G>A, p.R192H) (Fig. 1b), located in the cytosolic region of the C-terminal domain of Kir6.2. R192 is one of the positively charged donors in the three electrostatic interaction pairs (E229–R314, R301–E292 and R192–E227) between two adjacent subunits of Kir6.2, which are essential for stability of the Kir6.2 tetramer structure and pore-forming channel [25].

PSI-BLAST analysis demonstrated that Arg27 or Arg192 residues are evolutionally well-conserved in mammals, suggesting the functional importance of the two residues. Our proposed structure model (Fig. 2) indicates that R27 faces towards the interface of the Kir6.2 and SUR subunits, suggesting that R27H may have a greater influence on the interaction between Kir6.2 and SUR than R192H. Both R27H and R192H mutations show significant elevations in IC_{50} compared with the wild-type of Kir6.2, and R192H had a sevenfold lower sensitivity to ATP in vitro than R27H (Fig. 3a),

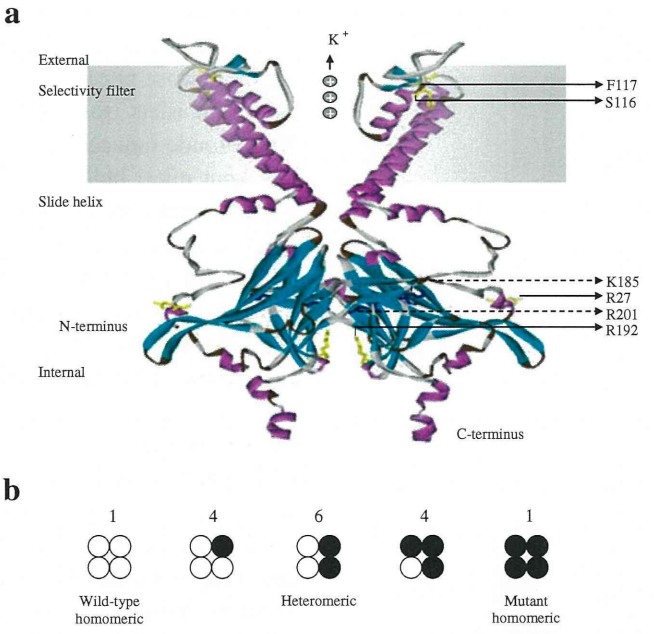

Fig. 2 Final modelled ribbon structure of two subunits of Kir6.2, indicating the location of the novel *KCNJ11* mutations. (**a**) The homology model of Kir6.2, which is quite similar to the previously reported structure of the other isoconformer, corresponds most closely to a truncated form of Kir6.2 expressed in the absence of SUR1. The labelled residues shown in yellow stick format are S116, F117, R27 and R192, which are indicated with solid arrows. The ATP-binding site is composed of the residues shown in the dark-blue stick model, R201 and K185, which are indicated with dashed arrows. (**b**) Schematic of the expected mixture of channels with different subunit compositions when wild-type and mutant Kir6.2 are coexpressed (as in the heterozygous state). The expected relative numbers of channel types for wild-type and mutant subunits are indicated above the figure, and segregate independently (i.e. follow a binomial distribution)

suggesting that both R27H and R192H reduce the sensitivity of the K_{ATP} channel to ATP-induced closure.

The index case from family c had a heterozygous frame shift mutation, causing deletion of Ser116 and Phe117 (NM_000525.3: c.348-353delCTTCTC, p.S116F117del), resulting in an in-frame deletion of two amino acid residues (Fig. 1c). Because no K_{ATP} currents were detected in the loss-of-function S116F117del channel in vitro, we did not further assay ATP sensitivity or sulfonylurea sensitivity for the S116F117del channel. The proposed structure model of Kir6.2 indicates that the evolutionally well-conserved Ser116 and Phe117 are residues located on the pore-forming H5 domain at the exit of the K_{ATP} channel on the TM region interface (Fig. 2). Ser116 lies within the end of the extracellular loop (94-116) connecting the TM region with the pore helix, H5; F117 lies at the beginning of the pore-forming helix (117-128) [9]. Deletion of these residues may compress the channel, preventing K^+ from flowing freely (Fig. 2), accounting for the absence of detectable currents as well as unregulated insulin secretion in vitro.

Hence the in-frame deletion loss-of-function mutation (p.S116F117del) probably primarily acts as a hyperinsulinism (HI) mutation.

Clinical characteristics of early-onset type 2 diabetic families with mutations We investigated the presence of these mutations in the probands' families. Of the five R27H carriers in family a, three had previously been diagnosed with diabetes. In addition, one was diagnosed with diabetes and one was diagnosed with IGT at the time of examination (Fig. 4 and Table 1); the average age of these newly diagnosed carriers at the time of diagnosis was 38.8 (range 32–52) years. These patients were prescribed insulin or gliclazide. None of the members of family a were obese. All R27H carriers had low serum insulin levels, and two (II-1 and II-2) patients who were treated with insulin had undetectable serum C-peptide (Table 1), indicating the absence of endogenous insulin secretion. Patients II-4 and III-2 were treated with a sulfonylurea alone (gliclazide), and achieved perfect control of their diabetes. In addition, a non-carrier, II-3 aged 51, had IGT. This individual most likely displays phenocopy, a phenomenon manifested in MODY pedigrees [17].

The tolbutamide sensitivity of the R27H, R192H and wild-type channels was not significantly different ($p>0.05$, Fig. 3b), suggesting that sulfonylureas could efficiently close the mutant channels and stimulate insulin secretion. Moreover, previous studies indicated that diabetic patients with a *KCNJ11* gain-of-function mutation could transfer successfully from insulin to oral sulfonylureas [26, 27]. As the affected R27H carriers in family a (II-4 or III-2) maintained perfect metabolic control with sulfonylureas, we adjusted the treatment of the other two R27H carriers (II-1 and II-2) from

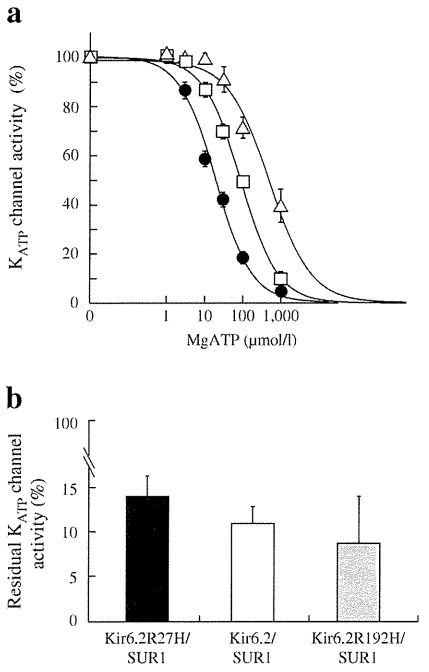

Fig. 3 ATP sensitivity and sulfonylurea sensitivity of the wild-type and mutant K_{ATP} channels. (**a**) ATP sensitivity. Patch-clamp experiments were performed for the wild-type (Kir6.2/SUR1, black circles, $n=10$) and mutant (Kir6.2 R27H/SUR1, white squares, $n=10$; Kir6.2 R192H/SUR1, white triangles, $n=8$) channels. The mutant channels had significantly higher IC_{50} values than the wild-type channels (92.3±9.6 vs 20.2±2.4 μmol/l, $p=2.66\times10^{-5}$; 652.7±178.0 vs 20.2±2.4 μmol/l, $p=9.14\times10^{-7}$), indicating that the mutant K_{ATP} channels had lower ATP sensitivities, especially the Kir6.2 R192H/SUR1 channel. (**b**) Sulfonylurea sensitivity. Residual K_{ATP} channel activities were determined by the ratio between the amplitudes of K_{ATP} channel currents before and after 100 μmol/l tolbutamide application. Experiments were conducted for wild-type (white column, $n=15$) and mutant (black column, Kir6.2 R27H/SUR1, $n=10$; Kir6.2 R192H/SUR1, grey column, $n=9$) channels. No significant difference in sulfonylurea sensitivity was observed for the mutant channels compared with the wild-type channels ($p>0.05$)

insulin to gliclazide, and these patients achieved good glycaemic control (HbA_{1c}, 5.7–6.4% [39–46 mmol/mol]).

In family b, four R192H carriers were previously diagnosed with diabetes; at the time of examination, their diabetes was treated with insulin or sulfonylureas (glimepiride) (Fig 4). Two R192H carriers (II-1 and III-1) were treated with insulin, with or without metformin, and had undetectable serum C-peptide (Table 1), indicating the absence of endogenous insulin secretion. The other two carriers (III-2 and III-3) were treated with sulfonylureas (glimepiride) with or without metformin, and maintained good control of their diabetes, suggesting that sulfonylureas are effective for R192H carriers with diabetes mellitus. We prescribed sulfonylurea therapy (glimepiride) for the other two R192H carriers (II-1 and III-1) who had been on insulin with metformin since diagnosis. Currently, these patients are only taking sulfonylureas and metformin, and their diabetes is well controlled (HbA_{1c}, 5.6–6.2% [38–44 mmol/mol] for II-1, 5.5–6.4% [37–46 mmol/mol] for III-1).

In family c, two S116F117del carriers had previously diagnosed diabetes (Fig. 4 and Table 1). Neither high concentration glucose nor tolbutamide elicits significant insulin secretion in islets isolated from Kir6.2 knockout mice [13]. Tolbutamide-induced insulin secretion is absent in Kir6.2 knockout mice, indicating that sulfonylurea-induced insulin secretion also critically depends on K_{ATP} channel activity. At the time of examination, S116F117del carrier II-1 had been effectively treated with insulin. The affected carriers of S116F117del were the proband III-1 (female, gestation 39 weeks, birthweight 4.0 kg, 95–97th percentile) [28], father II-1 (gestation 39 weeks, birthweight 3.8 kg, 75–90th percentile) and son IV-1 (gestation 38 weeks, birthweight 3.95 kg, 95–97th percentile). However, the unaffected sibling, brother III-2, a non-S116F117del carrier was in the normal range of birthweight (male, gestation 40 weeks, birthweight 3.3 kg, 25–50th percentile). In addition, all S116F117del carriers had complained that they had mild symptoms such as tremulousness, hunger and fatigue, which could be remitted by taking in food or glucose, when their blood glucose was determined to be 2.9–3.3 mmol/l (52.2–59.4 mg/dl) for proband III-1, 3.4–3.7 mmol/l (61.2–66.6 mg/dl) for son IV-1, and 3.6–3.9 mmol/l (64.8–70.2 mg/dl) for father II-1 during their childhood; this could be inferred to be largely due to mild hypoglycaemia caused by HI.

The clinical course of the proband III-1 was described as mild hypoglycaemia in childhood, IGT in early adulthood, and diabetes in middle age. Since diagnosis, this patient had been taking sulfonylureas without effective blood glucose control (HbA_{1c} 7.8–9.2% [62–77 mmol/mol]). Treatment of the patients was switched from sulfonylureas to insulin, at which point their blood glucose became normal and was well sustained (HbA_{1c} 5.2–6.3% [33–45 mmol/mol]). The son of this patient, IV-1, was on dietary control for IGT at the time of examination.

Discussion

Previous studies indicated that 90–95% of Chinese familial cases of early-onset type 2 diabetes remain genetically unexplained [29–31]. In this study, a 3.12% prevalence of *KCNJ11* mutations was observed in 96 Chinese families with early-onset type 2 diabetes mellitus, suggesting that *KCNJ11* may be one of the unidentified monogenic aetiologies in the Chinese population. Although three known *KCNJ11* variations were identified in the Chinese probands in this study, none had an association with familial early-onset type 2 diabetes mellitus. However, the E23K variation has been reported to be associated with modest reductions in ATP sensitivity and linked to type 2 diabetes mellitus [12, 32].

We demonstrated that two novel gain-of-function mutations (R27H and R192H) lead to the development of type 2

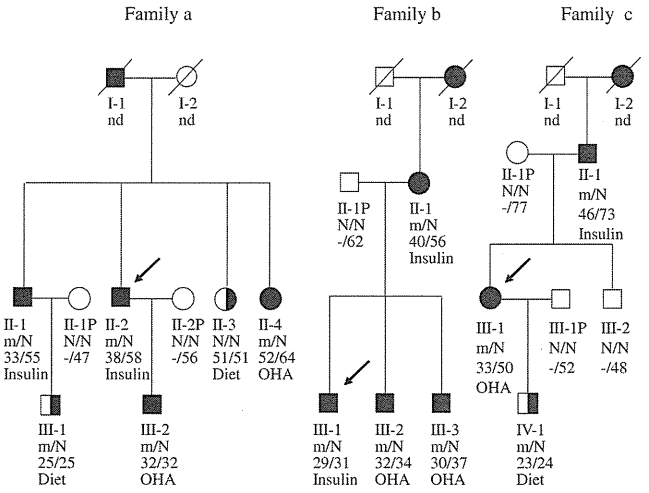

Fig. 4 Pedigrees, genotypes and clinical characteristics of families a, b and c. Black circles and squares indicate participants diagnosed with type 2 diabetes; half-filled black circles and squares indicate IGT; white circles and squares indicate normal glucose tolerance (NGT); black arrows indicate the index cases for the three families. Individuals treated with insulin did not undergo the OGTT. The numbers under the symbols are the family members' identification numbers, followed below by the genotype at codon 27 in family a, codon 192 in family b and codon 116-117 in family c, then age at diabetes diagnosis for affected members and age at examination, followed by treatment for diabetes. nd, not determined. Family a, Pedigree and genotypes of family a. Left pedigree shows the segregation of the R27H mutation. For the genotype, N shows normal allele (Arg); m shows mutant allele (His) at codon 27. The parametric LOD score for this pedigree was 0.83. OHA, oral hypoglycaemic agents, gliclazide. Family b, Pedigree and genotypes of family b. Middle pedigree shows the segregation of the R192H mutation. For the genotype, N shows normal allele (Arg); m shows mutant allele (His) at codon 192. The parametric $\log_{10}$ of odds (LOD) score for this pedigree was 0.60. OHA, glimepiride. Family c, Pedigree and genotypes of family c. Right pedigree shows the segregation of the S116F117del mutation. N shows normal allele S116F117; m shows mutant allele S116F117del (His) at codon116-117. The parametric LOD score for this pedigree was 0.52. OHA, gliclazide

diabetes by reducing the ATP-binding activity of Kir6.2. On comparison of the IC_{50} of the most common mutation, R201H [5], the mildest common variation, E23K [33], and the in-between mutation, C42R [6], with that of R192H or R27H, the reduction in ATP sensitivity is R201H>R192H>C42R>R27H>E23K, which is consistent with their clinical phenotypes in diabetes, i.e. the severe phenotype is PNDM, the mildest is type 2 diabetes and the

Table 1 Clinical characteristics of families a, b and c

Family	ID	Diagnosis	BMI (kg/m^2)	Glucose (mmol/l)		C-peptide (nmol/l)	Insulin (pmol/l)	
				FPG	2 h PG		FINS	2 h INS
a	II-1	DM	21.0	16.0	–	0.03	–	–
	II-2	DM	18.4	14.4	–	0.07	–	–
	II-4	DM	20.6	8.1	12.7	–	50.0	104.9
	III-1	IGT	20.3	5.1	8.1	–	61.8	200.0
	III-2	DM	21.0	5.9	11.5	–	43.1	134.0
b	II-1	DM	24.5	14.0	–	0.13	–	–
	III-1	DM	32.4	12.0	–	0.10	–	–
	III-2	DM	28.4	5.2	13.0	–	68.8	137.5
	III-3	DM	25.2	7.8	16.7	–	59.7	175.0
c	II-1	DM	23.6	7.2	11.8	0.13	–	–
	III-1	DM	26.2	8.3	13.1	–	41.0	150.0
	IV-1	IGT	22.8	5.8	8.2	–	55.6	224.3
166 cases		DM	24.3±3.4	9.5±4.1	15.4±4.8	0.70±0.05	127.8±97.2	304.2±192.4

Other clinical characteristics of the mutation carriers are shown. For comparison, means ± SD for the same characteristics in a group of 166 individuals with type 2 diabetes are shown. DM, diabetes mellitus; 2 h INS, 2 h plasma insulin; FINS, fasting plasma insulin; 2 h PG, 2 h plasma glucose; FPG, fasting plasma glucose

in-between is early-onset type 2 diabetes or MODY. Although these data suggest a strong genotype–phenotype relationship in *KCNJ11* mutations, the association is relative, not absolute. It has been reported that, in some families with the C42R or R201H mutation, the clinical presentation and degree of impaired beta cell function are different [5, 6, 34]. Even in families with R27H or R192H mutations, clinical symptoms in the same family were different. This suggests that both genetic and environmental factors may influence the clinical phenotypes, in addition to their responses to sulfonylureas.

One study reported that p.Glu227Lys (i.e. the E227K mutation) located at E227, a single amino acid that governs the electrostatic interaction of the R192–E227 pair, has a functional effect [25]. E227K reduces the ATP sensitivity of the K_{ATP} channel and increases the intrinsic open probability of the channel in its mutant heterozygous state in vitro [35]. In addition, several studies have indicated that the E227K mutation causes monogenic neonatal diabetes mellitus [35, 36]. Moreover, E227K has been identified as causal for a French MODY pedigree, and therefore the *KCNJ11* gene was proposed to be MODY13 in that study [7]. These E227K studies offer support for R192H, which caused MODY gene-negative autosomal dominantly inherited early-onset type 2 diabetes mellitus in family b, in the same way as E227K in the French MODY pedigree [7]. Further studies are required to confirm whether these effects occur in vivo.

We concluded that the development of type 2 diabetes in R27H and R192H carriers is due to defective glucose-induced insulin secretion via one of three distinct mechanisms: (1) primary impairment of the ATP sensitivity of the mutant K_{ATP} channels; (2) the effect of R27H on the interaction between Kir6.2 and SUR1 subunits in the K_{ATP} channel; (3) the effect of the mutant R192H on the stability of the Kir6.2 tetramer structure and the pore-forming channel.

Loss-of-function mutations in human SUR1/*ABCC8* or Kir6.2/*KCNJ11* are the most common causes of congenital HI of infancy [37, 38]. Patients with hyperinsulinaemic hypoglycaemia due to loss-of-function in K_{ATP}, such as heterozygous *ABCC8* mutations, 'cross-over' to diabetes in later life [39]. This is inferred from mouse models where loss-of-function in K_{ATP} channel activity led to glucose intolerance and diabetes on high-fat diets [14, 40].

The three affected heterozygous S116F117del carriers in family c were in the upper range of normal birthweight, suggesting that insulin oversecretion might have occurred in their fetal period. In addition, all S116F117del carriers with diabetes or IGT had mild symptoms of childhood hypoglycaemia in this study. Because of poor hospital conditions at the time, no insulin level tests were conducted in local hospitals, and we infer that they may have had HI during their childhood. Therefore the S116F117del mutation may represent a new subtype of autosomal dominantly inherited diabetes with a moderate phenotype, presenting as hyperinsulinaemic hypoglycaemia in childhood, IGT in early adulthood, and diabetes in middle age due to slow, progressive loss of insulin secretory capacity. Interestingly, one previously reported human *KCNJ11* mutation affecting S116 is known to be responsible for HI [41], which provides evidence to support the idea that p.S116F117del may have caused HI during childhood in family c (Fig. 4). However, the precise mechanism of the progressive loss of insulin secretory capacity and the reversion of the phenotype is still poorly understood.

Development of type 2 diabetes in S116F117del carriers was associated with defective glucose-induced insulin secretion, which promotes apoptotic beta cell death, and contributes to hyperglycaemia due to unregulated insulin secretion in later life.

As the residues S116, F117 and G132 are all located in the pore-forming domain of Kir6.2, the clinical course of human S116F117del mutation carriers may be similar to Kir6.2G132S transgenic mice [13], which exhibit hypoglycaemia and unregulated insulin secretion as neonates and then develop severe hyperglycaemia with almost no insulin response to glucose. A high frequency of apoptotic beta cells is observed before the appearance of hyperglycaemia in Kir6.2G132S transgenic mice, suggesting that K_{ATP} channels may play a significant role in beta cell survival, except for insulin secretion [14, 42]. Whether spontaneous regeneration of pancreatic beta cells can occur in human carriers of the S116F117del mutation, as in Kir6.2G132S transgenic mice, needs further investigation. Moreover, further experiments on S116F117del transgenic mice may help to explain HI or diabetes caused by this mutation, as well as the phenotype and mechanisms by which HI could result in diabetes in later life.

This study has enabled therapeutic improvements. Discontinuation of insulin and implementation of sulfonylureas for R27H or R192H carriers, and continuation/switch to insulin therapy for S116F117del carriers resulted in good control of glycaemic levels. Our results suggest that genetic diagnosis of the *KCNJ11* mutations in the autosomal dominantly inherited early-onset type 2 diabetic pedigrees may be helpful for understanding molecular aetiology and providing more personalised treatment for these specific forms of diabetes in Chinese individuals, as well as Asians patients in whom the prevalence of the investigated MODY genes [16] (i.e. *HNF4α/MODY1*, *GCK/MODY2*, *HNF1α/MODY3*, *PDX1/MODY4*, *HNF1β/MODY5* and *NEUROD1/MODY6*) is as low as 10–20% [30, 31, 43, 44].

Further studies are required to confirm whether these heterozygous mutations disturb pancreatic islet development or decrease beta cell mass. The identification of these novel mutations broadens the spectrum of diabetic phenotypes linked to *KCNJ11*, suggesting that routine genetic diagnosis for autosomal dominantly inherited early-onset type 2 diabetic families should also include *KCNJ11*.

Acknowledgements We thank Susumu Seino and Tadao Shibasaki (Division of Cellular and Molecular Medicine, Department of Physiology and Cell Biology, Kobe University Graduate School of Medicine, Japan), Nobuya Inagaki (Department of Diabetes and Clinical Nutrition, Kyoto University, Japan) and Long Yu (State Key Laboratory of Genetic Engineering, School of Life Sciences, Fudan University, China) for their cooperation. We also thank Weiping Jia, Xiaojing Ma, Ming Lu, Can Li, Weijing Zhao, Rong Zhang, Jun Yin, Yuqian Bao and Jing Xu (Shanghai Diabetes Institute, Department of Endocrinology & Metabolism, Shanghai Jiaotong University Affiliated Sixth People's Hospital, Shanghai, China) for their technical support and cooperation.

Funding This research was supported by grants from the Project of National Natural Science Foundation of China (nos. 81270876, 30771022 and 30971384) and the Shanghai Scientific & Technical Committee Foundation (nos. 10XD1403400 and 06ZR14051). YL is supported by NIH grant SC1DK087655.

Duality of interest The authors declare that there is no duality of interest associated with this manuscript.

Contribution statement All authors contributed to the conception and design, or analysis and interpretation of data, drafted the article or revised it critically for important intellectual content, and approved the final version to be published.

References

1. Bonnefond A, Froguel P, Vaxillaire M (2010) The emerging genetics of type 2 diabetes. Trends Mol Med 16:407–416
2. American Diabetes Association (2013) Diagnosis and classification of diabetes mellitus. Diabetes Care 36(Suppl 1):S67–S74
3. Fajans SS, Bell GI (2011) MODY: history, genetics, pathophysiology, and clinical decision making. Diabetes Care 34:1878–1884
4. Doria A, Yang Y, Malecki M et al (1999) Phenotypic characteristics of early-onset autosomal-dominant type 2 diabetes unlinked to known maturity-onset diabetes of the young (MODY) genes. Diabetes Care 22:253–261
5. Gloyn AL, Pearson ER, Antcliff JF et al (2004) Activating mutations in the gene encoding the ATP-sensitive potassium-channel subunit Kir6.2 and permanent neonatal diabetes. N Engl J Med 350:1838–1849
6. Yorifuji T, Nagashima K, Kurokawa K et al (2005) The C42R mutation in the Kir6.2 (KCNJ11) gene as a cause of transient neonatal diabetes, childhood diabetes, or later-onset, apparently type 2 diabetes mellitus. J Clin Endocrinol Metab 90:3174–3178
7. Bonnefond A, Philippe J, Durand E et al (2012) Whole-exome sequencing and high throughput genotyping identified KCNJ11 as the thirteenth MODY gene. PLoS One 7:e37423
8. Inagaki N, Gonoi T, Clement JP 4th et al (1995) Reconstitution of IKATP: an inward rectifier subunit plus the sulfonylurea receptor. Science 270:1166–1170
9. Tucker SJ, Gribble FM, Proks P et al (1998) Molecular determinants of KATP channel inhibition by ATP. EMBO J 17:3290–3296
10. Girard CA, Wunderlich FT, Shimomura K et al (2009) Expression of an activating mutation in the gene encoding the KATP channel subunit Kir6.2 in mouse pancreatic beta cells recapitulates neonatal diabetes. J Clin Invest 119:80–90
11. Proks P, Reimann F, Green N, Gribble F, Ashcroft F (2002) Sulfonylurea stimulation of insulin secretion. Diabetes 51(Suppl 3):S368–S376
12. Gloyn AL, Weedon MN, Owen KR et al (2003) Large-scale association studies of variants in genes encoding the pancreatic beta-cell KATP channel subunits Kir6.2 (KCNJ11) and SUR1 (ABCC8) confirm that the KCNJ11 E23K variant is associated with type 2 diabetes. Diabetes 52:568–572
13. Seino S, Iwanaga T, Nagashima K, Miki T (2000) Diverse roles of KATP channels learned from Kir6. 2 genetically engineered mice. Diabetes 49:311–318
14. Miki T, Tashiro F, Iwanaga T et al (1997) Abnormalities of pancreatic islets by targeted expression of a dominant-negative KATP channel. Proc Natl Acad Sci U S A 94:11969–11973
15. Fukui M, Nakano K, Obayashi H et al (1997) High prevalence of mitochondrial diabetes mellitus in Japanese patients with major risk factors. Metabolism 46:793–795
16. American Diabetes Association (2010) Diagnosis and classification of diabetes mellitus. Diabetes Care 33(Suppl 1):S62–S69
17. Yamagata K, Oda N, Kaisaki PJ et al (1996) Mutations in the hepatocyte nuclear factor-1alpha gene in maturity-onset diabetes of the young (MODY3). Nature 384:455–458
18. Yamagata K, Furuta H, Oda N et al (1996) Mutations in the hepatocyte nuclear factor-4alpha gene in maturity-onset diabetes of the young (MODY1). Nature 384:458–460
19. Froguel P, Zouali H, Vionnet N et al (1993) Familial hyperglycemia due to mutations in glucokinase: definition of a subtype of diabetes mellitus. N Engl J Med 328:697–702
20. Chèvre JC, Hani EH, Stoffers DA, Habener JF, Froguel P (1998) Insulin promoter factor 1 gene is not a major cause of maturity-onset diabetes of the young in French Caucasians. Diabetes 47:843–844
21. Beards F, Frayling T, Bulman M et al (1998) Mutations in hepatocyte nuclear factor 1beta are not a common cause of maturity-onset diabetes of the young in the U.K. Diabetes 47:1152–1154
22. Malecki MT, Jhala US, Antonellis A et al (1999) Mutations in NEUROD1 are associated with the development of type 2 diabetes mellitus. Nat Genet 23:323–328
23. The Expert Committee on the Diagnosis and Classification of Diabetes Mellitus (2003) Report of the Expert Committee on the Diagnosis and Classification of Diabetes Mellitus (position statement). Diabetes Care 26(Suppl 1):S5–S20
24. Pegan S, Arrabit C, Zhou W et al (2005) Cytoplasmic domain structures of Kir2.1 and Kir3.1 show sites for modulating gating and rectification. Nat Neurosci 8:279–287
25. Antcliff JF, Haider S, Proks P, Sansom MS, Ashcroft FM (2005) Functional analysis of a structural model of the ATP-binding site of the KATP channel Kir6.2 subunit. EMBO J 24:229–239
26. Nagano N, Urakami T, Mine Y et al (2012) Diabetes caused by Kir6.2 mutation: successful treatment with oral glibenclamide switched from continuous subcutaneous insulin infusion in the early phase of the disease. Pediatr Int 54:277–279
27. Pearson ER, Flechtner I, Njølstad PR et al (2006) Switching from insulin to oral sulfonylureas in patients with diabetes due to Kir6.2 mutations. N Engl J Med 355:467–477
28. Bonellie S, Chalmers J, Gray R, Greer I, Jarvis S, Williams C (2008) Centile charts for birthweight for gestational age for Scottish singleton births. BMC Pregnancy Childbirth 8:5
29. Ng MC, Lee SC, Ko GT et al (2001) Familial early-onset type 2 diabetes in Chinese patients: obesity and genetics have more significant roles than autoimmunity. Diabetes Care 24:663–671
30. Xu JY, Dan QH, Chan V et al (2005) Genetic and clinical characteristics of maturity-onset diabetes of the young in Chinese patients. Eur J Hum Genet 13:422–427
31. Liu L, Furuta H, Minami A et al (2007) A novel mutation, Ser159Pro in the NeuroD1/BETA2 gene contributes to the development of diabetes in a Chinese potential MODY family. Mol Cell Biochem 303:115–120
32. Villareal DT, Koster JC, Robertson H et al (2009) Kir6.2 variant E23K increases ATP-sensitive K+ channel activity and is associated with impaired insulin release and enhanced insulin sensitivity in adults with normal glucose tolerance. Diabetes 58:1869–1878

33. Schwanstecher C, Meyer U, Schwanstecher M (2002) Kir6.2 polymorphism predisposes to type 2 diabetes by inducing overactivity of pancreatic beta-cell ATP-sensitive K+ channels. Diabetes 51:875–879
34. Klupa T, Edghill EL, Nazim J et al (2005) The identification of a R201H mutation in KCNJ11, which encodes Kir6.2, and successful transfer to sustained-release sulphonylurea therapy in a subject with neonatal diabetes: evidence for heterogeneity of beta cell function among carriers of the R201H mutation. Diabetologia 8:1029–1031
35. Girard CA, Shimomura K, Proks P et al (2006) Functional analysis of six Kir6.2 (KCNJ11) mutations causing neonatal diabetes. Pflugers Arch 453:323–332
36. Flanagan SE, Patch AM, Mackay DJ et al (2007) Mutations in ATP-sensitive K+ channel genes cause transient neonatal diabetes and permanent diabetes in childhood or adulthood. Diabetes 56:1930–1937
37. Dunne MJ, Cosgrove KE, Shepherd RM, Aynsley-Green A, Lindley KJ (2004) Hyperinsulinism in infancy: from basic science to clinical disease. Physiol Rev 84:239–275
38. Loechner KJ, Akrouh A, Kurata HT et al (2011) Congenital hyperinsulinism and glucose hypersensitivity in homozygous and heterozygous carriers of Kir6.2 (KCNJ11) mutation V290M mutation: K(ATP) channel inactivation mechanism and clinical management. Diabetes 60:209–217
39. Huopio H, Otonkoski T, Vauhkonen I, Reimann F, Ashcroft FM, Laakso M (2003) A new subtype of autosomal dominant diabetes attributable to a mutation in the gene for sulfonylurea receptor 1. Lancet 361:301–307
40. Nichols CG, Koster JC, Remedi MS (2007) β-cell hyperexcitability: from hyperinsulinism to diabetes. Diabetes Obes Metab 9(Suppl 2): 81–88
41. Suchi M, MacMullen CM, Thornton PS et al (2006) Molecular and immunohistochemical analyses of the focal form of congenital hyperinsulinism. Mod Pathol 19:122–129
42. Oyama K, Minami K, Ishizaki K, Fuse M, Miki T, Seino S (2006) Spontaneous recovery from hyperglycemia by regeneration of pancreatic beta-cells in Kir6.2G132S transgenic mice. Diabetes 55:1930–1938
43. Hwang JS, Shin CH, Yang SW, Jung SY, Huh N (2006) Genetic and clinical characteristics of Korean maturity-onset diabetes of the young (MODY) patients. Diabetes Res Clin Pract 74:75–81
44. Plengvidhya N, Boonyasrisawat W, Chongjaroen N et al (2009) Mutations of maturity-onset diabetes of the young (MODY) genes in Thais with early-onset type 2 diabetes mellitus. Clin Endocrinol (Oxf) 70:847–853

Am J Physiol Endocrinol Metab 305: E585–E599, 2013.
First published July 2, 2013; doi:10.1152/ajpendo.00093.2013.

Dysfunctional mitochondrial bioenergetics and oxidative stress in Akita$^{+/Ins2}$-derived β-cells

Tanecia Mitchell,[1,2] Michelle S. Johnson,[1,2] Xiaosen Ouyang,[1,2,6] Balu K. Chacko,[1,2] Kasturi Mitra,[3] Xiaoyong Lei,[4] Ying Gai,[4] D. Ray Moore,[7] Stephen Barnes,[2,5,7] Jianhua Zhang,[1,2,6] Akio Koizumi,[8] Sasanka Ramanadham,[4] and Victor M. Darley-Usmar[1,2]

[1]Department of Pathology and [2]Center for Free Radical Biology, [3]Department of Genetics, [4]Department of Cell, Developmental, and Integrative Biology, and [5]Department of Pharmacology and Toxicology, University of Alabama at Birmingham, Birmingham, Alabama; [6]Birmingham Veterans Affairs Medical Center, Birmingham, Alabama; [7]Targeted Metabolomics and Proteomics Laboratory, University of Alabama at Birmingham, Birmingham, Alabama; and [8]Department of Health and Environmental Sciences, Kyoto Graduate School of Medicine, Kyoto, Japan

Submitted 19 February 2013; accepted in final form 1 July 2013

Mitchell T, Johnson MS, Ouyang X, Chacko BK, Mitra K, Lei X, Gai Y, Moore DR, Barnes S, Zhang J, Koizumi A, Ramanadham S, Darley-Usmar VM. Dysfunctional mitochondrial bioenergetics and oxidative stress in Akita$^{+/Ins2}$-derived β-cells. *Am J Physiol Endocrinol Metab* 305: E585–E599, 2013. First published July 2, 2013; doi:10.1152/ajpendo.00093.2013.—Insulin release from pancreatic β-cells plays a critical role in blood glucose homeostasis, and β-cell dysfunction leads to the development of diabetes mellitus. In cases of monogenic type 1 diabetes mellitus (T1DM) that involve mutations in the insulin gene, we hypothesized that misfolding of insulin could result in endoplasmic reticulum (ER) stress, oxidant production, and mitochondrial damage. To address this, we used the Akita$^{+/Ins2}$ T1DM model in which misfolding of the insulin 2 gene leads to ER stress-mediated β-cell death and thapsigargin to induce ER stress in two different β-cell lines and in intact mouse islets. Using transformed pancreatic β-cell lines generated from wild-type Ins2$^{+/+}$ (WT) and Akita$^{+/Ins2}$ mice, we evaluated cellular bioenergetics, oxidative stress, mitochondrial protein levels, and autophagic flux to determine whether changes in these processes contribute to β-cell dysfunction. In addition, we induced ER stress pharmacologically using thapsigargin in WT β-cells, INS-1 cells, and intact mouse islets to examine the effects of ER stress on mitochondrial function. Our data reveal that Akita$^{+/Ins2}$-derived β-cells have increased mitochondrial dysfunction, oxidant production, mtDNA damage, and alterations in mitochondrial protein levels that are not corrected by autophagy. Together, these findings suggest that deterioration in mitochondrial function due to an oxidative environment and ER stress contributes to β-cell dysfunction and could contribute to T1DM in which mutations in insulin occur.

diabetes mellitus; β-cell; mitochondrial respiration; endoplasmic reticulum stress; mitochondrial quality control

INSULIN RELEASE from pancreatic β-cells is largely dependent on mitochondrial and endoplasmic reticulum (ER) function and plays a critical role in maintaining blood glucose homeostasis. The synthesis of insulin in β-cells is an energy-requiring process, with as much as 50% of the total protein of these cells committed to generation of this single protein when stimulated (51). Insulin requires posttranslational processing before it is secreted, and it has been shown that mutations that lead to misfolding may cause neonatal diabetes (11, 51). Once considered rare, monogenic mutations in insulin are becoming recognized as causes of neonatal diabetes mellitus. They can also be causative factors for type 1b diabetes or maturity-onset diabetes of the young and in some cases early onset type 2 diabetes mellitus (T2DM) (27, 50). Mutations in the insulin gene lead to defective processing and accumulation of proinsulin in the ER, inducing ER stress. In addition, the consequent dysregulation of blood glucose homeostasis can initiate serious diabetic complications such as cardiovascular disease, neuropathy, and nephropathy (8). Thus, prevention or treatment of β-cell injury and diabetes mellitus onset/progression continues to be a challenge, particularly for the group of patients with mutations in the insulin gene.

It has been established that there is a potential link between the ER and the mitochondria, and this has been suggested to contribute to β-cell dysfunction in both type 1 diabetes mellitus (T1DM) and T2DM pathogenesis (3, 16, 43, 52, 58). One proposed sequence of events is that ER stress leads to disruption of Ca^{2+} flow to the mitochondria, causing mitochondrial dysfunction and triggering a series of cyclic events, such as oxidative stress, that culminates in induction of cell death (30). To counter the cell death processes and development of T1DM, prosurvival mechanisms such as autophagy can be initiated in β-cells (6). Autophagy is a multistep process that targets damaged proteins and organelles for degradation and efficiently regulates organelle turnover within the cell (57). The targeting of phagophores to dysfunctional mitochondria is dependent on mitochondrial quality and ubiquitinated proteins (17, 25). A decrease in mitochondrial quality can be identified by increased mitochondrial ROS production, mitochondrial fission, decreased membrane potential, mtDNA damage, and suppressed bioenergetic function (20). How mitochondrial morphology plays an important role in β-cell dysfunction is still unclear (52). In addition, how autophagy responds to metabolic stress and impacts bioenergetic function and cellular redox status is not well understood (26, 28, 47). This is important to understand since lack of degradation of damaged mitochondria can induce oxidative stress and cell death (20, 38).

As a means to identify mechanisms that contribute to T1DM and associated complications, several experimental models have been developed (4, 34, 49, 59). In particular, there are two animal models representative of the syndromes mentioned above known as the Munich *Ins2*^{C95S} mutant mouse (19) and the Akita$^{Ins2+/-}$ mouse (60). The Akita mouse model contains

Address for reprint requests and other correspondence: V. M. Darley-Usmar, Dept. of Pathology, Univ. of Alabama at Birmingham, Biomedical Research Bldg. II, 901 19th St. South, Birmingham, AL 35294 (e-mail: darley@uab.edu).